Derynck R, Akhurst RJ, Balmain A. (2001). TGF-beta signaling in tumor suppression and cancer progression. *Nat Genet* **29**: 117–129.

Derynck R, Zhang YE. (2003). Smad-dependent and Smad-independent pathways in TGF-beta family signalling. *Nature* **425**: 577–584.

Fashena SJ, Einarson MB, O'Neill GM, Patriotis C, Golemis EA. (2002). Dissection of HEF1-dependent functions in motility and transcriptional regulation. *J Cell Sci* **115**: 99–111.

Grönroos E, Hellman U, Heldin CH, Ericsson J. (2002). Control of Smad7 stability by competition between acetylation and ubiquitination. *Mol Cell* **10**: 483–493.

Hanyu A, Ishidou Y, Ebisawa T, Shimanuki T, Imamura T, Miyazono K. (2001). The N domain of Smad7 is essential for specific inhibition of transforming growth factor-beta signaling. *J Cell Biol* **155**: 1017–1027.

Hayashi H, Abdollah S, Qiu Y, Cai J, Xu YY, Grinnell BW *et al.* (1997). The MAD-related protein Smad7 associates with the TGFbeta receptor and functions as an antagonist of TGFbeta signaling. *Cell* **89**: 1165–1173.

Heldin CH, Miyazono K, ten Dijke P. (1997). TGF-beta signalling from cell membrane to nucleus through SMAD proteins. *Nature* **390**: 465–471.

Hynes RO. (1992). Integrins: versatility, modulation, and signaling in cell adhesion. *Cell* **69**: 11–25.

Ito Y, Zhao J, Mogharei A, Shuler CF, Weinstein M, Deng C *et al.* (2001). Antagonistic effects of Smad2 versus Smad7 are sensitive to their expression level during tooth development. *J Biol Chem* **276**: 44163–44172.

Iwata S, Souta-Kuribara A, Yamakawa A, Sasaki T, Shimizu T, Hosono O *et al.* (2005). HTLV-I Tax induces and associates with Crk-associated substrate lymphocyte type (Cas-L). *Oncogene* **24**: 1262–1271.

Juliano RL, Haskill S. (1993). Signal transduction from the extracellular matrix. *J Cell Biol* **120**: 577–585.

Kamiguchi K, Tachibana K, Iwata S, Ohashi Y, Morimoto C. (1999). Cas-L is required for beta 1 integrin-mediated costimulation in human Tcells. *J Immunol* **163**: 563–568.

Kato Y, Habas R, Katsuyama Y, Näär AM, He X. (2002). A component of the ARC/Mediator complex required for TGF beta/Nodal signalling. *Nature* **418**: 641–646.

Krishnan P, King MW, Neff AW, Sandusky GE, Bierman KL, Grinnell B *et al.* (2001). Human truncated Smad 6 (Smad 6s) inhibits the BMP pathway in *Xenopus laevis*. *Dev Growth Differ* **43**: 115–132.

Law SF, Estojak J, Wang B, Mysliwiec T, Kruh G, Golemis EA. (1996). Human enhancer of filamentation 1, a novel p130cas-like docking protein, associates with focal adhesion kinase and induces pseudohyphal growth in *Saccharomyces cerevisiae*. *Mol Cell Biol* **16**: 3327–3337.

Law SF, O'Neill GM, Fashena SJ, Einarson MB, Golemis EA. (2000). The docking protein HEF1 is an apoptotic mediator at focal adhesion sites. *Mol Cell Biol* **20**: 5184–5195.

Lee HY, Chun KH, Liu B, Wiehle SA, Cristiano RJ, Hong WK *et al.* (2002). Insulin-like growth factor binding protein-3 inhibits the growth of non-small cell lung cancer. *Cancer Res* **62**: 3530–3537.

Li L, Elledge SJ, Peterson CA, Bales ES, Legerski RJ. (1994). Specific association between the human DNA repair proteins XPA and ERCC1. *Proc Natl Acad Sci USA* **91**: 5012–5016.

Liu X, Elia AE, Law SF, Golemis EA, Farley J, Wang T. (2000). A novel ability of Smad3 to regulate proteasomal degradation of a Cas family member HEF1. *EMBO J* **19**: 6759–6769.

Minegishi M, Tachibana K, Sato T, Iwata S, Nojima Y, Morimoto C. (1996). Structure and function of Cas-L, a 105-kD Crk-associated substrate-related protein that is involved in beta 1 integrin-mediated signaling in lymphocytes. *J Exp Med* **184**: 1365–1375.

Miyake-Nishijima R, Iwata S, Saijo S, Kobayashi H, Kobayashi S, Souta-Kuribara A *et al.* (2003). Role of Crk-associated substrate lymphocyte type in the pathophysiology of rheumatoid arthritis in tax transgenic mice and in humans. *Arthritis Rheum* **48**: 1890–1900.

Nakao A, Afrakhte M, Morén A, Nakayama T, Christian JL, Heuchel R *et al.* (1997). Identification of Smad7, a TGFbeta-inducible antagonist of TGF-beta signalling. *Nature* **389**: 631–635.

Ohashi Y, Iwata S, Kamiguchi K, Morimoto C. (1999). Tyrosine phosphorylation of Crk-associated substrate lymphocyte-type is a critical element in TCR- and beta 1 integrin-induced T lymphocyte migration. *J Immunol* **163**: 3727–3734.

Ohashi Y, Tachibana K, Kamiguchi K, Fujita H, Morimoto C. (1998). T cell receptor-mediated tyrosine phosphorylation of Cas-L, a 105-kDa Crk-associated substrate-related protein, and its association of Crk and C3G. *J Biol Chem* **273**: 6446–6451.

Ohnuma K, Yamochi T, Uchiyama M, Nishibashi K, Yoshikawa N, Shimizu N *et al.* (2004). CD26 up-regulates expression of CD86 on antigen-presenting cells by means of caveolin-1. *Proc Natl Acad Sci USA* **101**: 14186–14191.

Pugacheva EN, Golemis EA. (2005). The focal adhesion scaffolding protein HEF1 regulates activation of the Aurora-A and Nek2 kinases at the centrosome. *Nat Cell Biol* **7**: 937–946.

Sasaki T, Iwata S, Okano HJ, Urasaki Y, Hamada J, Tanaka H *et al.* (2005). Nedd9 protein, a Cas-L homologue, is upregulated after transient global ischemia in rats: possible involvement of Nedd9 in the differentiation of neurons after ischemia. *Stroke* **36**: 2457–2462.

Seo S, Asai T, Saito T, Suzuki T, Morishita Y, Nakamoto T *et al.* (2005). Crk-associated substrate lymphocyte type is required for lymphocyte trafficking and marginal zone B cell maintenance. *J Immunol* **175**: 3492–3501.

Sugano Y, Matsuzaki K, Tahashi Y, Furukawa F, Mori S, Yamagata H *et al.* (2003). Distortion of autocrine transforming growth factor beta signal accelerates malignant potential by enhancing cell growth as well as PAI-1 and VEGF production in human hepatocellular carcinoma cells. *Oncogene* **22**: 2309–2321.

Tachibana K, Urano T, Fujita H, Ohashi Y, Kamiguchi K, Iwata S *et al.* (1997). Tyrosine phosphorylation of Crk-associated substrates by focal adhesion kinase. A putative mechanism for the integrin-mediated tyrosine phosphorylation of Crk-associated substrates. *J Biol Chem* **272**: 29083–29090.

Tanaka J, Miwa Y, Miyoshi K, Ueno A, Inoue H. (1999). Construction of Epstein–Barr virus-based expression vector containing mini-oriP. *Biochem Biophys Res Commun* **264**: 938–943.

van Seventer GA, Salmen HJ, Law SF, O'Neill GM, Mullen MM, Franz AM *et al.* (2001). Focal adhesion kinase regulates beta1 integrin-dependent T cell migration through an HEF1 effector pathway. *Eur J Immunol* **31**: 1417–1427.

Vojtek AB, Hollenberg SM, Cooper JA. (1993). Mammalian Ras interacts directly with the serine/threonine kinase Raf. *Cell* **74**: 205–214.

Xu L, Chen YG, Massagué J. (2000a). The nuclear import function of Smad2 is masked by SARA and unmasked by TGFbeta-dependent phosphorylation. *Nat Cell Biol* **2**: 559–562.

Xu W, Angelis K, Danielpour D, Haddad MM, Bischof O, Campisi J *et al.* (2000b). Ski acts as a co-repressor with Smad2 and Smad3 to regulate the response to type beta transforming growth factor. *Proc Natl Acad Sci USA* **97**: 5924–5929.

Yagil C, Hubner N, Monti J, Schulz H, Sapojnikov M, Luft FC *et al.* (2005). Identification of hypertension-related genes through an integrated genomic-transcriptomic approach. *Circ Res* **96**: 617–625.

Zhang Z, Baron R, Horne WC. (2000). Integrin engagement, the actin cytoskeleton, and c-Src are required for the calcitonin-induced tyrosine phosphorylation of paxillin and HEF1, but not for calcitonin-induced Erk1/2 phosphorylation. *J Biol Chem* **275**: 37219–37223.

Supplementary Information accompanies the paper on the Oncogene website (http://www.nature.com/onc).

Anti-CD26 Monoclonal Antibody–Mediated G_1-S Arrest of Human Renal Clear Cell Carcinoma Caki-2 Is Associated with Retinoblastoma Substrate Dephosphorylation, Cyclin-Dependent Kinase 2 Reduction, $p27^{kip1}$ Enhancement, and Disruption of Binding to the Extracellular Matrix

Teruo Inamoto,[1,3] Tadanori Yamochi,[1] Kei Ohnuma,[1] Satoshi Iwata,[1] Shinichiro Kina,[1] Sakiko Inamoto,[1,3] Masaaki Tachibana,[2] Yoji Katsuoka,[3] Nam H. Dang,[4] and Chikao Morimoto[1,4]

Abstract

Purpose: CD26 is a 110-kDa cell surface glycoprotein with a role in tumor development through its association with key intracellular proteins. In this report, we show that binding of soluble anti-CD26 monoclonal antibody (mAb) inhibits the growth of the human renal carcinoma cells in both *in vitro* and *in vivo* experiments.

Experimental Design: Growth inhibition by anti-CD26 mAb was assessed using proliferation assay and cell cycle analysis. Anti-CD26 mAb, chemical inhibitors, dominant-negative, or constitutively active forms of specific signaling molecules were used to evaluate CD26-associated pathways. The *in vivo* growth-inhibitory effect of anti-CD26 mAb was also assessed in a human renal carcinoma mouse xenograft model.

Results: *In vitro* experiments show that anti-CD26 mAb induces G_1-S cell cycle arrest associated with enhanced $p27^{kip1}$ expression, down-regulation of cyclin-dependent kinase 2, and dephosphorylation of retinoblastoma substrate. Moreover, our data show that enhanced $p27^{kip1}$ expression is dependent on the attenuation of Akt activity. Anti-CD26 mAb also internalizes cell surface CD26, leading to decreased binding to collagen and fibronectin. Experiments with a mouse xenograft model involving human renal carcinoma cells show that anti-CD26 mAb treatment drastically inhibits tumor growth in tumor-bearing mice, resulting in enhanced survival.

Conclusions: Taken together, our data strongly suggest that anti-CD26 mAb treatment may have potential clinical use for CD26-positive renal cell carcinomas.

CD26 is a 110-kDa surface glycoprotein with dipeptidyl peptidase IV activity able to cleave selected biological factors to alter their functions (1). CD26/dipeptidyl peptidase IV is involved in T lymphocyte signal transduction processes (2, 3) and regulates topoisomerase IIα level in hematologic malignancies, affecting sensitivity to doxorubicin and etoposide (4). Moreover, our previous work showed that anti-CD26 monoclonal antibody (mAb) inhibits growth of CD26-positive T-cell malignancies (5, 6). Expressed on various tissues, including epithelial cells of liver, intestine, and kidney (1, 7), CD26 is involved in the development of certain human cancers, with lung adenocarcinomas, differentiated thyroid carcinomas, and metastatic prostate cancer being CD26 high and other histologic types of lung carcinomas, benign thyroid diseases, and primary prostate cancer being CD26 low (7–10). Notably, the role of CD26 in cancer biology depends on tumor types, as it is associated with high level of tumor aggressiveness in some and lower level in others (7–10). In a previous report, CD26 expression was detected on renal cell carcinoma (RCC) with unclear clinical significance (11). Extending these previous findings, we now define CD26 expression on normal and malignant tubular epithelial kidney tissues and establish that CD26 is an appropriate target for RCC treatment.

CD26 structure consists of three regions, an extracellular region, a 22-residue hydrophobic transmembrane region, and a 6-amino acid cytoplasmic region. The extracellular region contains a membrane-proximal glycosylated domain, a cysteine-rich domain, and a 260-amino acid COOH-terminal domain containing dipeptidyl peptidase IV activity. We now

Authors' Affiliations: [1]Division of Clinical Immunology, Advanced Clinical Research Center, Institute of Medical Science, University of Tokyo; [2]Department of Urology, Tokyo Medical College, Tokyo, Japan; [3]Department of Urology, Osaka Medical College, Osaka, Japan; and [4]Department of Hematologic Malignancies, Nevada Cancer Institute, Las Vegas, Nevada

Received 2/16/06; revised 3/22/06; accepted 3/29/06.

Grant support: Grant-in-Aid of Ministry of Education, Science, Sports, and Culture (K. Ohnuma and C. Morimoto) and Ministry of Health, Labor, and Welfare, Japan (C. Morimoto); Osaka Kidney Foundation grant OKF05-0002 (T. Inamoto); and The Yasuda Medical Foundation.

The costs of publication of this article were defrayed in part by the payment of page charges. This article must therefore be hereby marked *advertisement* in accordance with 18 U.S.C. Section 1734 solely to indicate this fact.

Requests for reprints: Chikao Morimoto, Division of Clinical Immunology, Advanced Clinical Research Center, Institute of Medical Science, University of Tokyo, 4-6-1, Shirokanedai, Minato-ku, Tokyo 108-8639, Japan. Phone: 81-3-5449-5549; Fax: 81-3-5449-5548; E-mail: morimoto@ims.u-tokyo.ac.jp.

doi:10.1158/1078-0432.CCR-06-0361

show that the anti-CD26 mAb 14D10, which recognizes the cell membrane-proximal glycosylated region starting with a 20-amino acid flexible stalk region of human CD26, induces cell cycle arrest, concomitantly blocking the adhesion of RCC cells to the extracellular matrix (ECM). In addition, anti-CD26 mAb-mediated growth arrest of RCC cells results from dephosphorylation of retinoblastoma substrate, decreased level of cyclin-dependent kinase (CDK) 2, and up-regulation of the Akt-dependent CDK inhibitor $p27^{kip1}$. Furthermore, studies using a mouse xenograft model show that anti-CD26 mAb treatment inhibits RCC tumor growth *in vivo*. Our work hence suggests a potential role for CD26-targeted therapy in the treatment of human RCC.

Materials and Methods

Reagents and antibodies. Anti-CD26 mAb (IgG1) 14D10 and anti-CD45 mAb (IgG1) 2H4 were developed in our laboratory as described previously (12, 13), with the latter being used as isotype-matched control mAb. Rabbit mAb to Thr^{308} or Ser^{473}-phosphorylated forms of Akt and phosphorylated extracellular signal-regulated kinase (ERK) 1/2 and mouse mAb to protein kinase Bα/Akt, ERK1/2, CDK4, CDK6, and phosphothreonine were from Cell Signaling Technology, Inc. (Beverly, MA), and mouse mAb to $p21^{cip1/waf1}$, CDK2, p53, cyclin D1, retinoblastoma substrate, and $p27^{kip1}$ were from BD PharMingen (Lexington, KY). Oct-1, and α-tubulin were from Santa Cruz Biotechnology (Santa Cruz, CA). LY294002, wortmannin, and PD98059 were from Calbiochem (San Diego, CA). Nocodazole was from Sigma-Aldrich (St. Louis, MO). Nocodazole (500 ng/mL from 1 mg/mL stock solution in DMSO), LY294002 (30 μmol/L from 50 mmol/L stock solution in DMSO), and PD98059 (30 μmol/L from 10 mmol/L stock solution in DMSO) were added to the culture medium 30 minutes before treatment with each antibody.

Cell culture and transfection procedures. Caki-2 (human renal carcinoma), LNCap (androgen-dependent prostate carcinoma), and DU-145 cells (androgen-independent prostate carcinoma) were kind gifts from Dr. Haruhito Azuma (Osaka Medical College, Osaka, Japan). VMRC-RCW (human renal carcinoma), Caki-1 (human renal carcinoma), and ACHN (human renal carcinoma) were obtained from Cell Resource Center for Biomedical Research (Tohoku University, Sendai, Japan). All cells were grown in RPMI 1640 (Life Technologies, Inc., Grand Island, NY) supplemented with 10% heat-inactivated fetal bovine serum, penicillin (100 units/mL), and streptomycin (100 μg/mL; Life Technologies, Inc., Gaithersburg, MD) or G418 (500 μg/mL; Sigma-Aldrich). The plasmid vectors (Upstate Biotechnology, Lake Placid, NY) used in exploring signaling pathway were as follows: the Myc-tagged NH_2-terminal myristylated active Akt1 cDNA (Myr-Akt), dominant-negative form of Akt cDNA (d.n.-Akt), and hemagglutinin-tagged constitutive active mitogen-activated protein kinase (MAPK)/ERK kinase (MEK) 1 cDNA (upstream of 44/42MAPK; c.a. MEK1), with all three constructs being placed in a pUSEamp vector. The plasmids were transfected into various cells using Fugene 6 reagent (Roche Diagnostics, Indianapolis, IN). In each experiment, neomycin phosphotransferase II (Upstate Biotechnology) was probed to evaluate transfection efficacy.

Cell cycle analyses. Cells (1×10^6 per well) were incubated in medium alone or in the presence of anti-CD26 or isotype-matched control mAbs at indicated concentrations in the presence or absence of nocodazole. DNA contents were analyzed using propidium iodide as described previously (5) and were measured using FACSCalibur (Becton Dickinson Co., San Jose, CA) with CellQuest software (Becton Dickinson) and ModFit program (Becton Dickinson). In all experiments, at least $>1 \times 10^4$ cells were sorted after gating out the fixation artifacts and cell debris.

2-(2-Methoxy-4-nitrophenyl)-3-(4-nitrophenyl)-5-(2,4-disulfophenyl)-2H-tetrazolium assay. Cells were synchronized using double-thymidine block method as described previously (14), then released, and subjected to incubation in 96-well plates in medium alone or in the presence of anti-CD26 (0.1, 1, or 10 μg/mL) or isotype-matched control mAbs (0.1, 1, or 10 μg/mL) for a total volume of 100 μL (5×10^3 cells per well). After 24 hours of incubation in 37°C, 2-(2-methoxy-4-nitrophenyl)-3-(4-nitrophenyl)-5-(2,4-disulfophenyl)-2H-tetrazolium (Seikagaku, Tokyo, Japan) was added to each well. After another 2 hours of incubation, water-soluble formazan dye on bioreduction in the presence of an electron carrier, 1-methoxy-5-methylphenazinium, was measured at 450 nm using a microplate reader (Bio-Rad, Hercules, CA). All samples were tested in triplicate. Values reported represent the mean of triplicated wells, and SE was within 15%.

Immunocytochemistry and immunohistochemistry. For fluorescent microscopy experiments, cells were treated and stained according to the methods described previously (3). In brief, Caki-2 cells (5×10^4/mL) were grown on coverslips in six-well plates in the presence or absence of anti-CD26 mAb. The cells were fixed in 4% paraformaldehyde followed by permeabilization with 0.1% Triton X-100 in PBS and stained with anti-$p27^{kip1}$ mAb and FITC-conjugated anti-mouse IgG (Jackson ImmunoResearch, West Grove, PA). After mounting with a ProLong Antifade kit (Molecular Probes, Eugene, OR), slides were examined by Olympus IX70 confocal microscope with 40 objective lenses (Olympus, Tokyo, Japan) using laser excitation at 488 nm. For immunohistochemistry, 11 primary RCC surgical specimens from patients were evaluated. For each, 10% formalin-fixed, paraffin-embedded specimens containing both the carcinoma and its adjacent nonneoplastic tissue were prepared. Slides were deparaffinized and then heated in a microwave processor for antigen retrieval in 10 mmol/L citrate buffer (pH 6) for 10 minutes. After blocking in 3% (v/v) bovine serum albumin, slides were incubated at 4°C overnight with the primary antibody (anti-CD26 mAb), washed with PBS, incubated for 30 minutes with FITC-conjugated anti-mouse IgG, and then analyzed using confocal laser microscopy. To serve as a control for nonspecific staining, duplicate sections were stained with isotype-matched mAb instead of the primary antibody. Two different pathologists checked the validity of the obtained results. All human specimens were obtained from the Department of Urology, Tokyo Medical College (Tokyo, Japan), and informed consents were obtained from all patients according to the format of the Institutional Review Board.

SDS-PAGE and immunoblotting. Preparation of whole-cell lysates and cell fractionations were done as described elsewhere (15). For detection of phosphorylated proteins, cells were harvested in NP40 buffer [1% NP40, 0.5% sodium deoxycholate, 5 mmol/L EDTA, 50 mmol/L Tris-HCl (pH 8), 0.15 mol/L NaCl] containing 1 mmol/L phenylmethylsulfonyl fluoride, 10 mmol/L NaF, 1 mmol/L Na_3VO_4, 10 μg/mL aprotinin, and 10 μg/mL leupeptin. The protein samples were subjected to SDS-PAGE and transferred to polyvinylidene difluoride membrane (Immobilon-P, Millipore, Bedford, MA). Specific antigens were probed by the corresponding mAbs followed by horseradish peroxidase–conjugated secondary Ig (Amersham Pharmacia Biotech, Piscataway, NJ). Western blots were visualized by the enhanced chemiluminescence technique (NEN, Boston, MA).

In vivo *model.* *In vivo* studies were approved by the Institute Animal Care and Use Committee. Female-specific pathogen-free BALB/c nu−/− mice (ages 8 weeks) were purchased from Charles River (Yokohama, Japan). All mice were pretreated by i.p. route with 0.2 mL anti-asialo-GM1 polyclonal antisera (25%, v/v; Wako, Osaka, Japan) 1 day before tumor transplant to eliminate host natural killer cell activity. For a xenograft model of RCC, mice were anesthetized with diethyl ether and subjected to direct s.c. inoculation of Caki-2 cells (1×10^6 per mouse) in 100 μL Matrigel (BD Biosciences, San Jose, CA). The studies involving the observation of tumor volume and survival advantage included five mice per group. Mice bearing established tumors (~5 mm in size) received PBS alone, anti-CD26 mAb, or isotype-matched control mAb by intratumoral injection in 0.1-mL volume of sterile PBS at 10 μg per

dose as described previously (6). The mice were injected every 4 days for 60 days. Tumor-bearing mice were then monitored for tumor development and progression. Tumor size was determined by caliper measurement of the largest (x) and smallest (y) perpendicular diameters every 4 days and calculated according to the formula $V = \pi/6 \times xy^2$. Cumulative proportion survival was assessed by Kaplan-Meier. Necropsies of moribund mice were done for evaluation of tumor, and tumors were removed to be frozen. After homogenization by Dounce homogenizer, frozen tissues were lysed in lysis buffer [1% SDS, 4 mol/L urea, 1 mmol/L EDTA, 150 mmol/L NaCl, 50 mmol/L Tris (pH 8)]. Each 50 μg of lysates was subjected to SDS-PAGE and immunoblotting to examine protein levels of $p27^{kip1}$, phosphorylated Akt, and β-actin.

Results

Cell surface CD26 is highly expressed on human RCC. Previous work showed CD26 expression is enhanced on RCC (11). We first evaluated CD26 expression level on surgically resected human RCC tissues from Japanese patients. Eleven consecutive surgically resected RCC specimens from the primary sites were examined for surface CD26 expression. CD26 was highly expressed on RCC tissues compared with normal renal cells surrounding the RCC (Fig. 1A, *a* and *b*) particularly in normal proximal tubules (Fig. 1A, *c* and *d*). All 11 RCC tissues and 6 normal renal tissues surrounding RCC were evaluated for their CD26 expression intensity, revealing high expression on human RCC tissues compared with normal renal tissues (Fig. 1B). The RCC cell lines Caki-2, VMRC-RCW, Caki-1, and ACHN all exhibited high surface CD26 levels, with DU-145 and LNCap showing much lower expression (Fig. 1C). These data indicated that all RCC cells tested were highly CD26 positive, whereas tumor cells arising from other origins, including prostate cancers, exhibited much lower level.

Anti-CD26 mAb induces cell cycle arrest at G_1-S checkpoint and growth inhibition of RCC. Because we showed previously that anti-CD26 mAb treatment induced cell cycle arrest at G_1-S in CD26-positive T-cell lymphoma and T-cell clones (5, 6), we first examined anti-CD26 mAb effect on cell cycle progression of CD26-positive RCC cell lines. Treatment of Caki-2 cells with anti-CD26 blocked cell cycle progression at G_1-S (Fig. 2A), an effect better visualized when cells were treated with nocodazole to induce M-phase cell cycle arrest (Fig. 2B). Caki-2 cells exhibited a significant increase in G_0-G_1 from 14 to 28 hours after initiation of anti-CD26 treatment (Fig. 2C), whereas

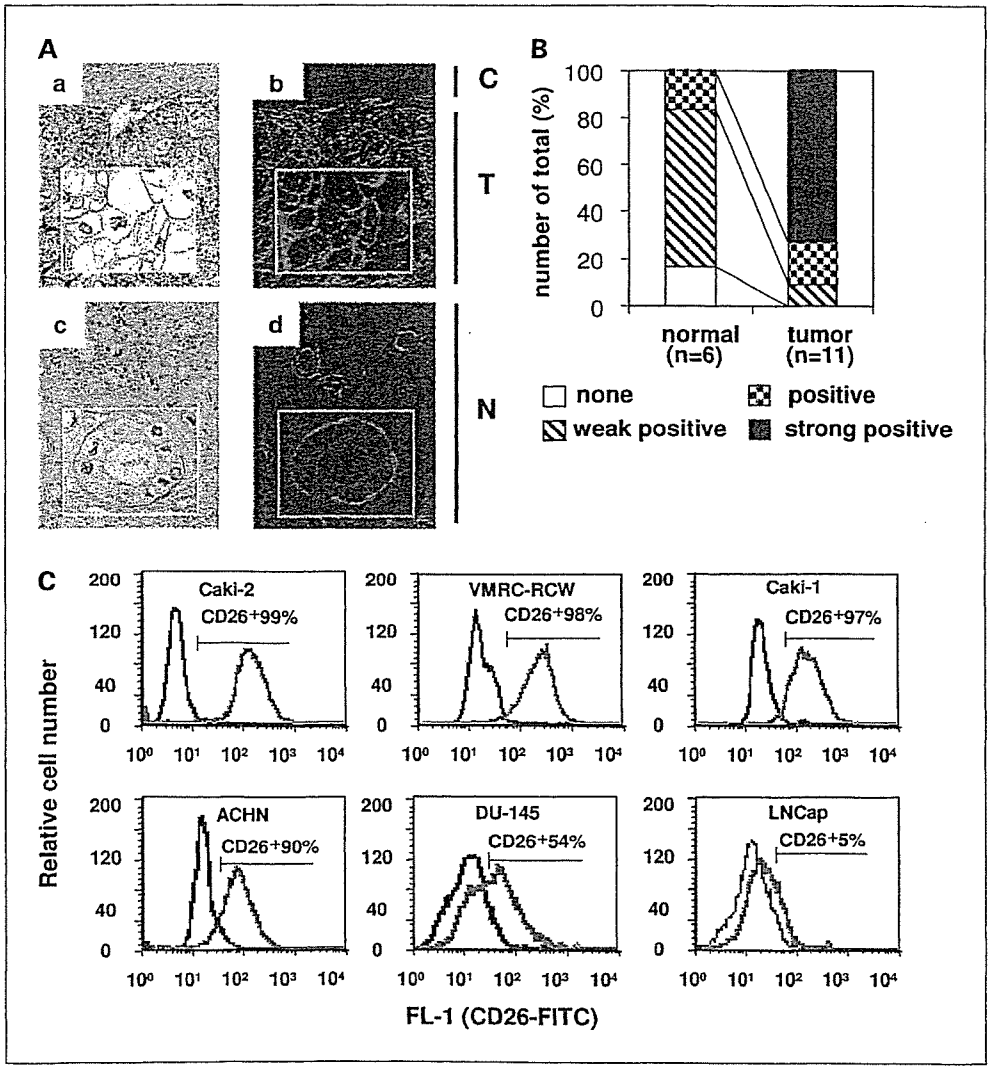

Fig. 1. Cell surface expression of CD26 in human RCC. *A*, immunohistochemical analysis of CD26 expression was done on surgically resected RCC specimens of primary sites. RCC stained with H&E (*a*) and anti-CD26-FITC (*b*). Normal renal structures adjacent to RCC tissues in (*a*) and (*b*) were stained with H&E (*c*) and anti-CD26-FITC (*d*). Representative of 11 consecutive specimens. Original magnification, ×200. *N*, normal renal tissue; *C*, connective tissue; *T*, tumor. *B*, fluorescent intensities of CD26 were evaluated from 11 RCC tissue samples and 6 adjacent normal renal tissues. Fluorescent intensity was determined as follows: strong positive (*T*; Fig. 1A, *b*), positive (Fig. 1A, *d*), weak positive (*C*; Fig. 1A, *b*), or none. Identical experiments were repeated thrice with similar results. *C*, surface expression of CD26 on various cell lines was analyzed by flow cytometry. Red line, CD26 histograms were obtained by staining with mouse anti-CD26 mAb followed by staining with rabbit anti-mouse IgG-FITC conjugate. Black line, control histograms represent background fluorescence obtained by staining of same cell cultures with isotype-matched control mAb.

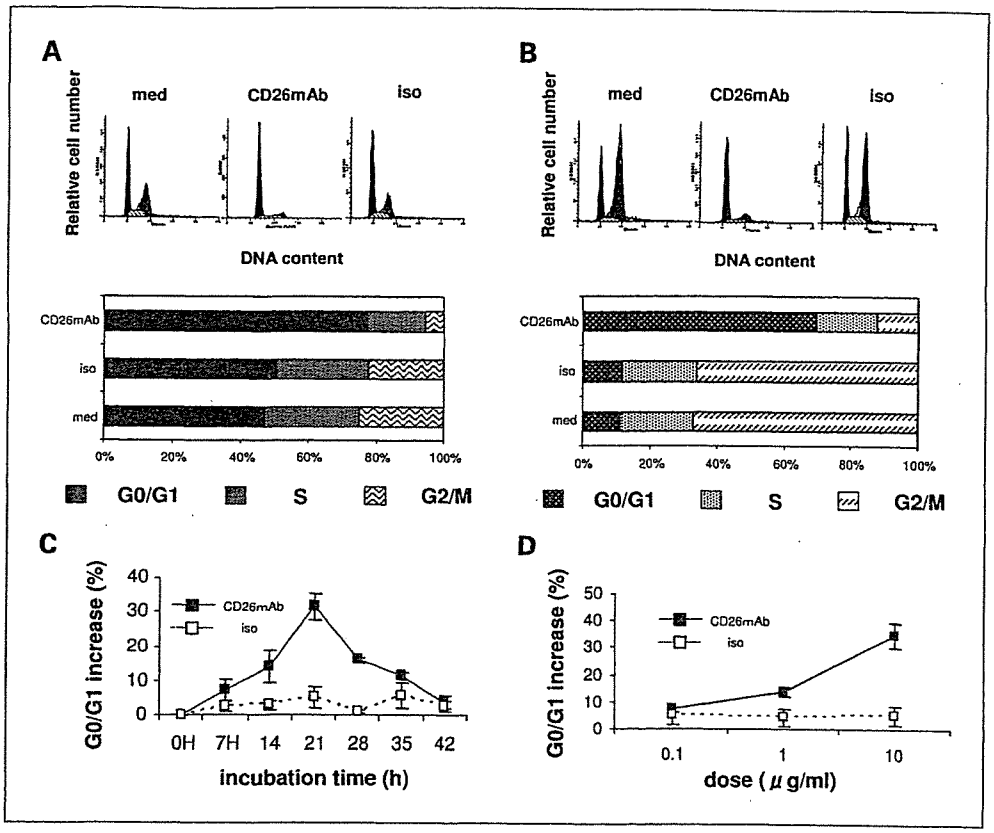

Fig. 2. Anti-CD26 mAb-mediated cell cycle arrest at G_1-S checkpoint in RCC. *A*, Caki-2 cells were treated with medium alone (*med*), anti-CD26 mAb (*CD26mAb*), or isotype-matched control mAb (*iso*) for 21 hours, and cell cycle analysis was done by ModFit program. Histograms were made by CellQuest software. Data are representative of three independent experiments. *B*, nocodazole was added to Caki-2 cells 30 minutes before administration of medium, anti-CD26 mAb, or isotype-matched control mAb. Data are representative of three independent experiments. *C*, Caki-2 cells were treated with isotype-matched control mAb or anti-CD26 mAb. After the indicated time period, cell cycle analysis was done. Points, mean of triplicated tests; bars, SE. *D*, Caki-2 cells were treated with isotype-matched control mAb or anti-CD26 mAb at a concentration of 0.1, 1, and 10 μg/mL. Caki-2 cells were collected for cell cycle analysis at 21 hours after antibody administration.

anti-CD26 mAb-mediated G_0-G_1 arrest occurred in a dose-dependent manner, peaking at 10 μg/mL (Fig. 2D). Consistent with the observed anti-CD26 mAb-induced cell cycle arrest G_1-S, growth of Caki-2, VMRC-RCW, Caki-1, ACHN, and DU-145 cells was inhibited in a dose-dependent manner when treated with anti-CD26 mAb for 24 hours (Fig. 3). However, anti-CD26 mAb had minimal growth-inhibitory effect on LNCap cells, indicating the specific antitumor effect of anti-CD26 mAb.

Enhancement of $p27^{kip1}$ expression, reduction of CDK2, and dephosphorylation of retinoblastoma substrate are associated with anti-CD26 mAb-mediated G_1-S cell cycle arrest through phosphatidylinositol 3-kinase/Akt and ras/raf/MEK/ERK(MAPK) pathways. Because the cell cycle is strictly regulated by regulators (16), we next evaluated the levels of cell cycle regulators in Caki-2 cells following anti-CD26 mAb treatment. Enhanced expression of $p27^{kip1}$, reduction of CDK2, and dephosphorylation of retinoblastoma substrate were observed, with no detectable changes in $p21^{cip/waf1}$, p53, cyclin D1, CDK4, and CDK6 (Fig. 4A). Markedly enhanced $p27^{kip1}$ level was detected in the nuclei of anti-CD26-treated cells (Fig. 4B), corroborated by results of cell fractionation study (Fig. 4C). Moreover, immunoprecipitation analysis with anti-$p27^{kip1}$ mAb revealed that anti-CD26 mAb treatment reduced the amount of phosphothreonine residue of $p27^{kip1}$, suggesting that accumulation of $p27^{kip1}$ is nuclei specific (Fig. 4D; ref. 17). These results strongly suggested that anti-CD26-mediated up-regulation of $p27^{kip1}$ occurred mainly in the nucleus, being potentially responsible for cell cycle arrest in RCC.

Because anti-CD26 mAb induced nuclear accumulation of $p27^{kip1}$ protein, concomitantly reducing the phosphorylated form of $p27^{kip1}$ (Fig. 4B-D), we hypothesized that the phosphatidylinositol 3-kinase/Akt pathway is involved in this process (17, 18). Elucidating the particular signaling pathways involved in anti-CD26 mAb-mediated up-regulation of $p27^{kip1}$, we found that activated Akt was significantly abrogated in Caki-2 cells as early as 7 hours and as late as 21 hours after antibody treatment (Fig. 5A, *b, lanes 16-21*). Attenuation of 44/42MAPK

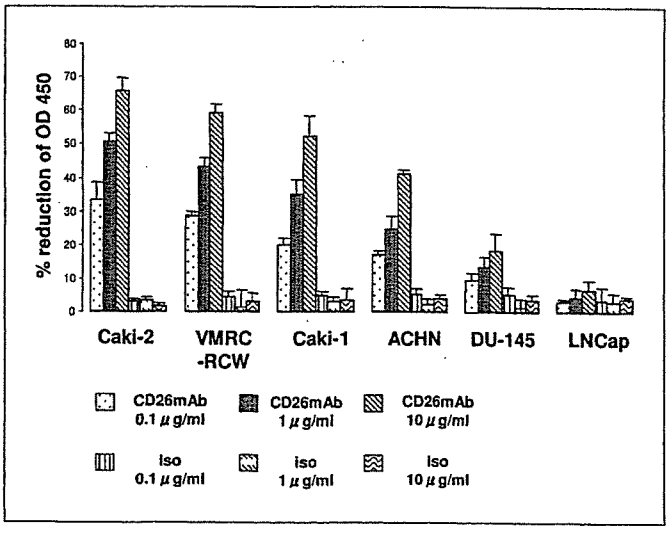

Fig. 3. Inhibitory effect of anti-CD26 mAb on RCC proliferation. Synchronized 5×10^3 cells per well of Caki-2, VMRC-RCW, Caki-1, ACHN, DU-145, and LNCap were incubated in 96-well plates in the presence of either anti-CD26 or isotype-matched control mAbs. After 24 hours of antibody treatment, water-soluble formazan dye on bioreduction in the presence of an electron carrier, 1-methoxy-5-methylphenazinium, was measured at 450 nm using a microplate reader as described in Materials and Methods, and growth-inhibitory ratio was calculated as % reduction of $A_{450\ nm}$.

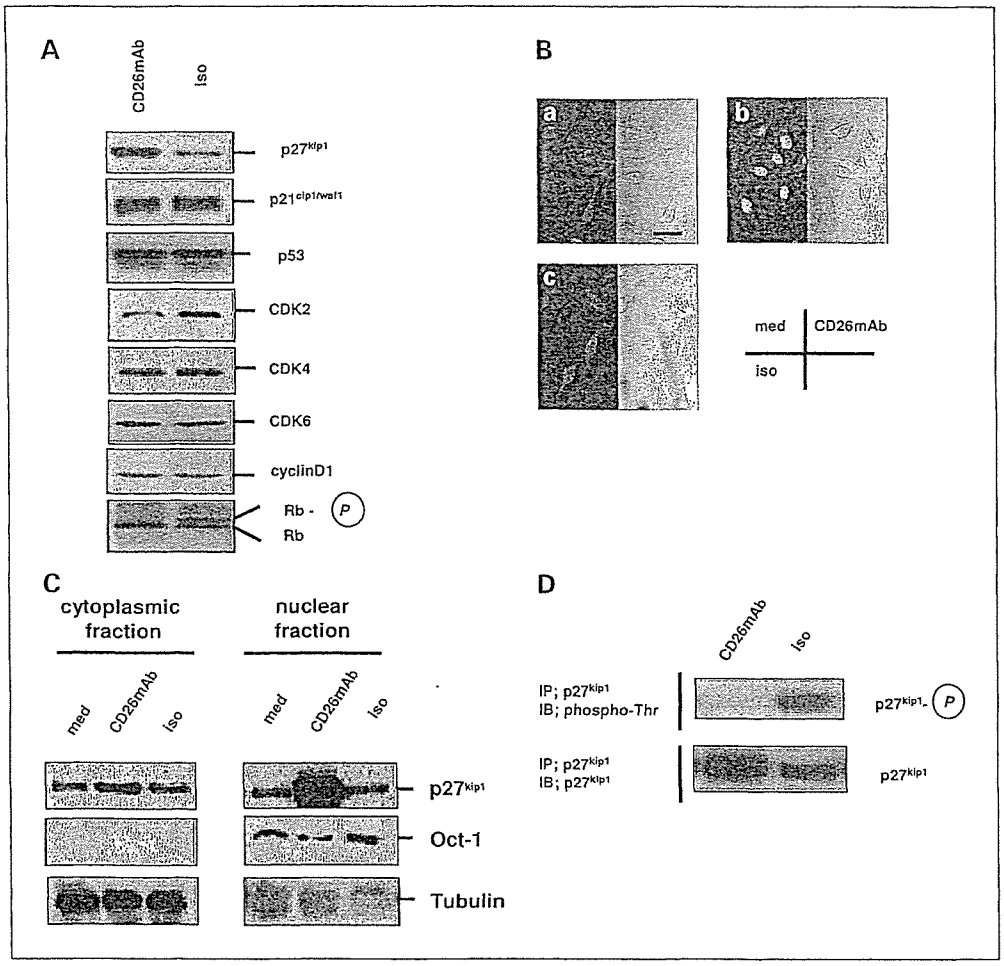

Fig. 4. Anti-CD26 mAb-mediated induction of $p27^{kip1}$ expression. *A*, Caki-2 cells were treated with medium alone, anti-CD26 mAb, or isotype-matched control mAb. At 21 hours after antibody administration, cells were harvested, lysed, subjected to SDS-PAGE, and probed by specific antibody to $p27^{kip1}$, $p21^{cip1/waf1}$, p53, CDK2, CDK4, CDK6, cyclin D1, and phosphorylated retinoblastoma substrate (*Rb*). *B*, Caki-2 cells (5×10^4/mL) were grown on coverslips in six-well plates in medium alone (*a*), anti-CD26 mAb (*b*), or isotype-matched control mAb (*c*). After 21 hours of incubation, cells were subjected to immunocytochemistry as described in Materials and Methods and stained with mouse anti-$p27^{kip1}$ mAb followed by FITC-conjugated anti-mouse IgG. Bar, 50 μm. *C*, after 21 hours of treatment with medium alone, anti-CD26 mAb, or isotype-matched control mAb, Caki-2 cells were harvested for cell fractionation. Each sample was probed with antibodies against $p27^{kip1}$. To determine fractionation purity, Oct-1 and α-tubulin were probed with specific antibodies for cytoplasmic and nuclear fractions, respectively. *D*, for immunoprecipitation, whole-cell lysates were precipitated with anti-$p27^{kip1}$ mAb, subjected to SDS-PAGE, and probed by specific antibody to phosphothreonine.

was also observed as late as 21 hours following antibody treatment of Caki-2 cells (Fig. 5A, *d, lanes 19-21*).

To further characterize the specific pathway with a key role in the anti-CD26 mAb-induced enhancement of $p27^{kip1}$ expression, specific inhibitors against each pathway as well as genetically introduced His/Myc-tagged dominant-negative form of Akt (Caki-2-d.n.-Akt) and constitutively active His/Myc-tagged myristylated Akt (Caki-2-myr-Akt) were used (Fig. 5B-D). Caki-2 pretreated with LY294002 (Fig. 5B, *e, lanes 3, 6,* and *9*) and Caki-2-d.n.-Akt (Fig. 5C, *a, lanes 7-9*) up-regulated endogenous $p27^{kip1}$ protein level, more importantly resulting in additive up-regulation of $p27^{kip1}$ when combined with anti-CD26 mAb. In contrast, Caki-2-myr-Akt exhibited only sparse basal level of $p27^{kip1}$, completely abolishing anti-CD26 mAb-induced up-regulation of $p27^{kip1}$ (Fig. 5C, *a, lanes 10-12*). Meanwhile, PD98059, a specific inhibitor of MEK1, did not cause any detectable change in $p27^{kip1}$ (Fig. 5B, *e, lanes 2, 5,* and *8*). These findings strongly suggested that the phosphatidylinositol 3-kinase/Akt pathway is more potent than the ras/raf/MEK/ERK pathway in mediating anti-CD26 mAb-induced $p27^{kip1}$ accumulation.

To confirm the above results, Caki-2 pretreated with LY294002 and PD98059, Caki-2-d.n.-Akt, and Caki-2-myr-Akt were evaluated for cell proliferation activity. Caki-2 pretreated with LY294002 and Caki-2-d.n.-Akt displayed drastically increased anti-CD26 mAb-mediated growth inhibition, whereas Caki-2-myr-Akt completely abolished this effect (Fig. 5D). On the other hand, pretreatment of Caki-2 with PD98059 did not enhance anti-CD26 mAb-mediated growth inhibition. Taken together, the above results showed that the phosphatidylinositol 3-kinase/Akt pathway was more potent than the ras/raf/MEK/ERK pathway in regulating anti-CD26 mAb-mediated growth arrest and that Akt activity has an effect on anti-CD26 mAb-induced expression of $p27^{kip1}$ and growth arrest.

Anti-CD26 mAb regulates cell adhesion to ECM through internalization of cell surface CD26 and reduces in vivo *tumorigenicity of Caki-2 associated with prolonged survival.* Because CD26 plays a role in cell adhesion to the ECM proteins (19, 20), we examined the effect of anti-CD26 mAb on cellular interaction with the ECM. Anti-CD26 antibody inhibited Caki-2 binding to fibronectin and type I collagen (Fig. 6A) associated with antibody-mediated CD26 internalization (Fig. 6B). These findings thus suggested that contact inhibition may play a contributing role to the observed anti-CD26-mediated up-regulation of $p27^{kip1}$ (21, 22).

We also investigated the effect of anti-CD26 mAb treatment on Caki-2 growth in a xenograft mouse tumor model. Mice treated with anti-CD26 mAb had a lower rate of tumor development than controls, leading to enhanced survival (Fig. 6C). To define the molecular events occurring in inoculated tumors, tumor mass was removed at day 60 after initial treatment for postmortem biochemical analyses of tissue lysates. Our results showed enhanced expression of $p27^{kip1}$ protein with

concomitant inactivation of Akt in the tumor mass (Fig. 6D), consistent with our *in vitro* data (Figs. 4 and 5). Taken together, these results indicated that CD26 may be an appropriate molecular target for RCC therapy.

Discussion

In this study, we show the antitumor effect of anti-CD26 mAb in an *in vitro* and *in vivo* model. Importantly, our study suggests the potential role of CD26 as a molecular target in human RCC, a highly malignant disease that is resistant to standard treatment with chemotherapy or biologics (23). Although highly expressed in RCC, particularly the clear cell type (11), CD26 role in human RCC is poorly understood. Our present results indicate that anti-CD26 mAb induces RCC G_1-S cell cycle and growth inhibition, concomitantly blocking cell adhesion. Our data also suggest that targeting CD26 is a potentially effective therapeutic strategy for selected neoplasms, including human RCC. Of interest is that tumors can result from cell cycle dysregulation, with various cancers expressing low levels of CDK inhibitors, including $p27^{kip1}$ (16).

Although recent work showed that activated Akt regulates both $p27^{kip1}$ subcellular localization and degradation (17, 24), we show that combining anti-CD26 mAb with LY294002 or a dominant-negative form of Akt has an additive effect on $p27^{kip1}$ accumulation. In contrast, constitutively active Akt abolishes not only basal $p27^{kip1}$ protein level but also anti-CD26 mAb-induced $p27^{kip1}$ overexpression, with resultant amelioration of growth inhibition by anti-CD26 mAb. These observed results strongly suggest that Akt negatively regulates total $p27^{kip1}$ protein level, and perturbation of CD26 by its specific antibody engages the same pathway in RCC, leading to an increase in G_0-G_1 phase. Meanwhile, the mechanisms involved in anti-CD26 mAb-induced inactivation of Akt resulting in $p27^{kip1}$ accumulation in RCC remain to be elucidated. One possible explanation may involve the potential interaction between CD26 and the docking sites for Akt. Binding of anti-CD26 antibody causes CD26 internalization, leading to signal transduction. Because Akt is a lipid-binding protein kinase, which becomes activated as a result of recruitment to docking

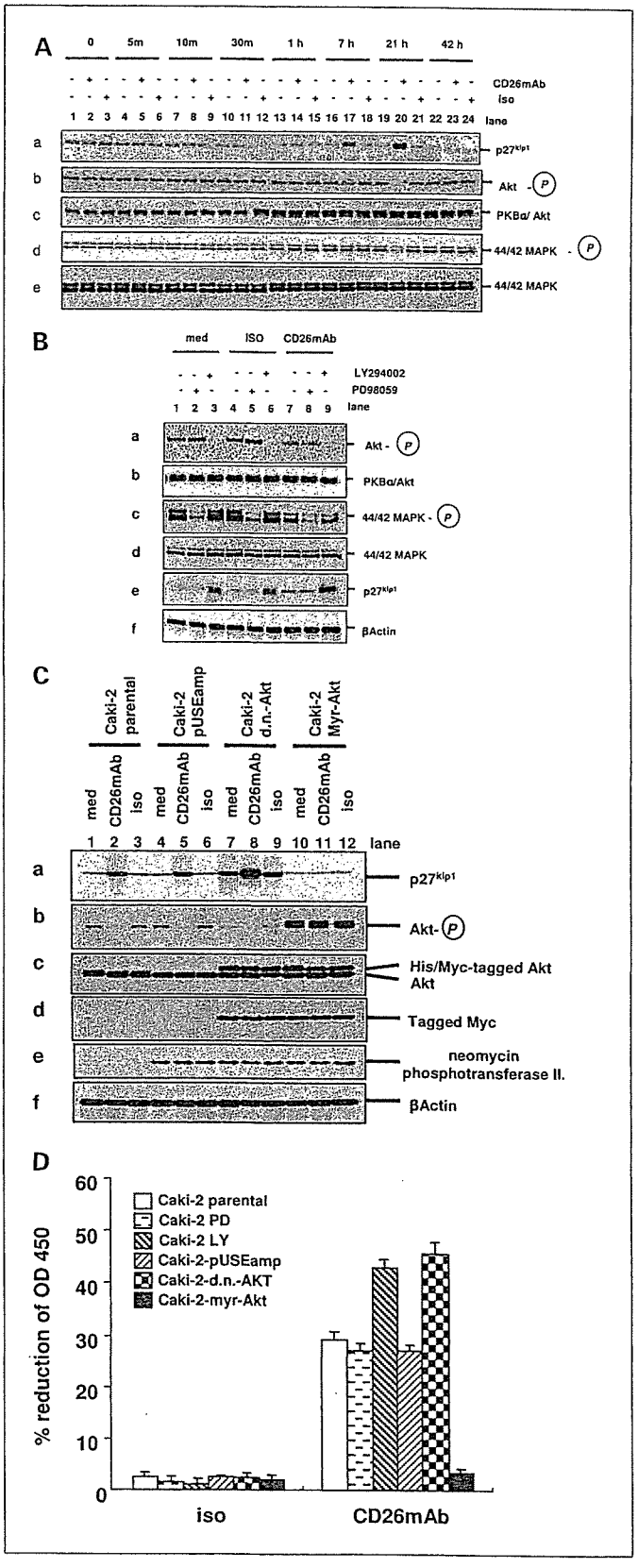

Fig. 5. Anti-CD26 mAb-mediated enhancement of $p27^{kip1}$ in RCC via attenuation of phosphorylated Akt rather than phosphorylated 44/42MAPK. *A*, Caki-2 cells were treated with medium only, anti-CD26 mAb, or isotype-matched control mAb. Caki-2 cells were immediately collected for preparation of whole-cell lysates at 0, 5, 10, and 30 minutes and 1, 7, 21, and 42 hours after administration of indicated panel of antibodies. *B*, for whole-cell lysate preparation, Caki-2 cells were preincubated in the presence or absence of PD98059 and LY294002 30 minutes before treatment with medium alone, isotype-matched control mAb, or anti-CD26 mAb at 10 μg/mL. After 21 hours of antibody treatment, cells were harvested and subjected to SDS-PAGE and immunoblotting for $p27^{kip1}$ (*a*), phosphorylated Akt (*b*), protein kinase Bα/Akt (*c*), phosphorylated 44/42MAPK (*d*), 44/42MAPK (*e*), and β-actin (*f*). *C*, SDS-PAGE and immunoblotting of whole-cell lysates of Caki-2 cells that express a His/Myc-tagged dominant-negative Akt (Caki-2-d.n.-Akt), His/Myc-tagged myristylated constitutively active Akt (Caki-2-myr-Akt), and control vector (Caki-2-pUSEamp). Transient transfectants of Caki-2-pUSEamp, Caki-2-d.n.-Akt, and Caki-2-myr-Akt were made, and after 48 hours, each of the three transfectants was treated by medium alone, 10 μg/mL anti-CD26 mAb, or 10 μg/mL isotype-matched control mAb. Twenty-one hours after antibody treatment, cells were collected, lysed, subjected to SDS-PAGE and immunoblotting, and probed with specific antibody to $p27^{kip1}$ (*a*), phosphorylated Akt (*b*), protein kinase Bα/Akt (*c*), Myc (*d*), neomycin phosphotransferase II (*e*), and β-actin (*f*). *D, in vitro* proliferation assay of Caki-2-parental, Caki-2 pretreated by PD98059, Caki-2 pretreated by LY294002, Caki-2-pUSEamp, Caki-2-d.n.-Akt, and Caki-2-myr-Akt. Caki-2 cells were preincubated in the presence or absence of PD98059 (*Caki-2 PD*) and LY294002 (*Caki-2 LY*) for 30 minutes before treatment with isotype-matched control or anti-CD26 mAbs. Transient transfectants of Caki-2-pUSEamp, Caki-2-d.n.-Akt, and Caki-2-myr-Akt were established 48 hours before treatment with isotype-matched control mAb or anti-CD26 mAb. Anti-CD26 and isotype-matched control mAbs were administered at 10 μg/mL to each cell type, and then cells were subjected to *in vitro* cell proliferation assay. Independent tests were examined in triplicates. Columns, mean; bars, SE.

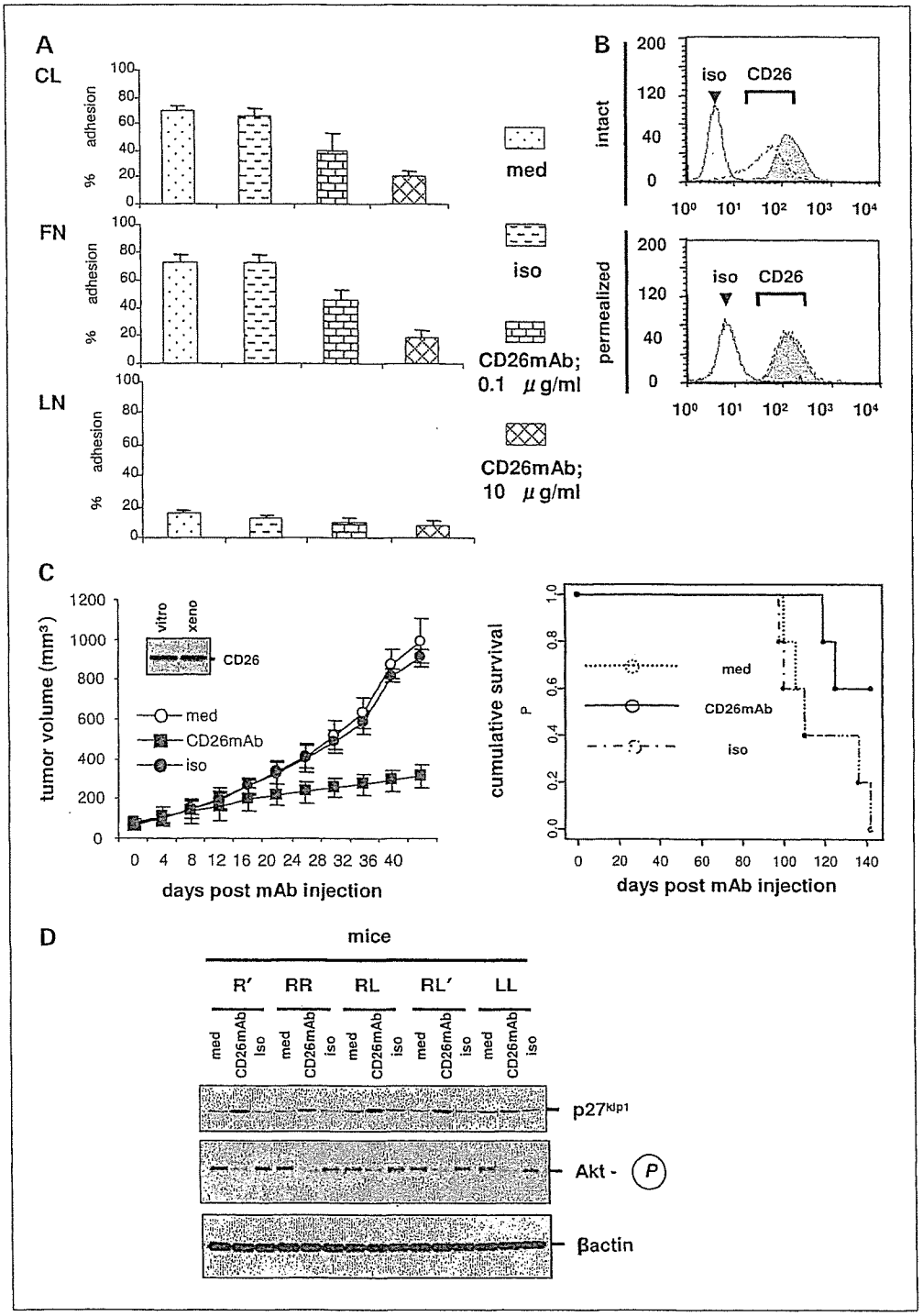

Fig. 6. Antitumor effect of anti-CD26 mAb in mouse xenograft model of Caki-2. *A*, effect of anti-CD26 mAb on cell adhesion to ECM. Caki-2 cells treated with medium only, anti-CD26 mAb, or isotype-matched control mAb were plated onto 60-mm dishes (3×10^6 per dish) coated with collagen I (*CL*), fibronectin (*FN*), or laminin (*LN*) and cultured for 21 hours. The adhesive ability of cancer cells was expressed as the mean number of cells that had attached to the bottom surface of the dish. Columns, mean number of cells per field of view; bars, SE. Values for invasion were determined by calculating the average number of adhesive cells per mm^2 over three fields per assay and expressed as an average of triplicate determinations. Adhesive cells (%): adhesive cells / adhesive cells + nonadhesive cells. *B*, Caki-2 cells were treated with anti-CD26 mAb on ice, or isotype-matched control mAb, followed by washing in ice-cold PBS twice and subsequently incubated at 37°C for 12 hours. Cell were collected and stained with FITC-conjugated anti-mouse IgG. Expression status of cell surface CD26 was analyzed by flow cytometry. To detect total CD26 level, including the internalized CD26 fraction, cell membrane permeabilization method was used (26). Filled histogram, positive control, which was incubated 30 minutes with anti-CD26 mAb. Open histogram, status of CD26 after treatment. *C*, Caki-2 cells (1×10^6) were inoculated s.c. into the left flank of mice. CD26 expression of Caki-2 cells after tumor implantation into the mouse was similar to its level before tumor implantation. Mice were treated with intratumoral injection of PBS only (medium; $n = 5$), anti-CD26 mAb ($n = 5$), or isotype-matched control mAb ($n = 5$) on the day when the tumor mass became visible (5 mm in size). Tumor size and cumulative survival were monitored. *D*, resected specimens were immediately frozen for whole-cell lysate preparation and lysed by lysis buffer as described in Materials and Methods. Protein (50 μg) was applied for SDS-PAGE and immunoblotting for $p27^{kip1}$, phosphorylated Akt, and β-actin. R′, RR, RL, RL′, and LL, names of mice in each treatment group.

sites consisting of phosphatidylinositol phosphate in the plasma membrane (25), antibody-induced CD26 internalization may affect Akt docking and activation in RCC. Moreover, because anti-CD26 mAb blocks ECM binding and because $p27^{kip1}$ is up-regulated during contact inhibition (21), anti-CD26 mAb may induce cellular mechanisms associated with contact inhibition in selected CD26-positive adhesive tumors.

Our present study shows that CD26 is highly expressed in human RCC and that anti-CD26 mAb binding engages key signaling pathways, resulting in G_1-S arrest. Our subsequent *in vivo* experiments further indicate that CD26 is an appropriate molecular target for RCC therapy by showing that anti-CD26 mAb treatment leads to loss of tumorigenicity. We postulate that the potent antitumor effect of anti-CD26 mAb observed in our study may be used in the future as novel therapeutic approaches against various CD26-positive malignancies, including RCC.

Acknowledgments

We thank Y. Urasaki and Y. Itoh for their technical assistance.

References

1. Morimoto C, Schlossman SF. The structure and function of CD26 in the T-cell immune response. Immunol Rev 1998;161:55–70.
2. Ishii T, Ohnuma K, Murakami A, et al. CD26-mediated signaling for T cell activation occurs in lipid rafts through its association with CD45RO. Proc Natl Acad Sci U S A 2001;98:12138–43.
3. Ohnuma K, Yamochi T, Uchiyama M, et al. CD26 up-regulates expression of CD86 on antigen-presenting cells by means of caveolin-1. Proc Natl Acad Sci U S A 2004;101:14186–91.
4. Yamochi T, Yamochi T, Aytac U, et al. Regulation of p38 phosphorylation and topoisomerase IIα expression in the B-cell lymphoma line Jiyoye by CD26/dipeptidyl peptidase IV is associated with enhanced *in vitro* and *in vivo* sensitivity to doxorubicin. Cancer Res 2005;65:1973–83.
5. Ohnuma K, Ishii T, Iwata S, et al. G_1/S cell cycle arrest provoked in human T cells by antibody to CD26. Immunology 2002;107:325–33.
6. Ho L, Aytac U, Stephens LC, et al. *In vitro* and *in vivo* antitumor effect of the anti-CD26 monoclonal antibody 1F7 on human $CD30^+$ anaplastic large cell T-cell lymphoma Karpas 299. Clin Cancer Res 2001;7:2031–40.
7. Pro B, Dang NH. CD26/dipeptidyl peptidase IV and its role in cancer. Histol Histopathol 2004;19:1345–51.
8. Iwata S, Morimoto C. CD26/dipeptidyl peptidase IV in context. The different roles of a multifunctional ectoenzyme in malignant transformation. J Exp Med 1999;190:301–6.
9. Kehlen A, Lendeckel U, Dralle H, Langner J, Hoang-Vu C. Biological significance of aminopeptidase N/CD13 in thyroid carcinomas. Cancer Res 2003;63:8500–6.
10. Kajiyama H, Kikkawa F, Suzuki T, Shibata K, Ino K, Mizutani S. Prolonged survival and decreased invasive activity attributable to dipeptidyl peptidase IV overexpression in ovarian carcinoma. Cancer Res 2002;62:2753–7.
11. Droz D, Zachar D, Charbit L, Gogusev J, Chrétein Y, Iris L. Expression of the human nephron differentiation molecules in renal cell carcinomas. Am J Pathol 1990;137:895–905.
12. Morimoto C, Torimoto Y, Levinson G, et al. 1F7, a novel cell surface molecule, involved in helper function of CD4 cells. J Immunol 1989;143:3430–9.
13. Kobayashi S, Ohnuma K, Uchiyama M, et al. Association of CD26 with CD45RA outside lipid rafts attenuates cord blood T-cell activation. Blood 2004;103:1002–10.
14. Blajeski AL, Phan VA, Kottke TJ, Kaufmann SH. G(1) and G(2) cell-cycle arrest following microtubule depolymerization in human breast cancer cells. J Clin Invest 2002;110:91–9.
15. Sato K, Aytac U, Yamochi T, et al. CD26/dipeptidyl peptidase IV enhances expression of topoisomerase IIα and sensitivity to apoptosis induced by topoisomerase II inhibitors. Br J Cancer 2003;89:1366–74.
16. Sherr CJ. Principles of tumor suppression. Cell 2004;116:235–46.
17. Shin I, Yakes FM, Rojo F, et al. PKB/Akt mediates cell-cycle progression by phosphorylation of p27 (Kip1) at threonine 157 and modulation of its cellular localization. Nat Med 2002;8:1145–52.
18. Viglietto G, Motti ML, Bruni P, et al. Cytoplasmic relocalization and inhibition of the cyclin-dependent kinase inhibitor p27(Kip1) by PKB/Akt-mediated phosphorylation in breast cancer. Nat Med 2002;8:1136–44.
19. Cheng HC, Abdel-Ghany M, Pauli BU. A novel consensus motif in fibronectin mediates dipeptidyl peptidase IV adhesion and metastasis. J Biol Chem 2003;278:24600–7.
20. Dang NH, Torimoto Y, Schlossman SF, Morimoto C. Human CD4 helper T cell activation: functional involvement of two distinct collagen receptors, 1F7 and VLA integrin family. J Exp Med 1990;172:649–52.
21. Suzuki E, Nagata D, Yoshizumi M, et al. Reentry into the cell cycle of contact-inhibited vascular endothelial cells by a phosphatase inhibitor. Possible involvement of extracellular signal-regulated kinase and phosphatidylinositol 3-kinase. J Biol Chem 2000;275:3637–44.
22. Levenberg S, Yarden A, Kam Z, Geiger B. p27 is involved in N-cadherin-mediated contact inhibition of cell growth and S-phase entry. Oncogene 1999;18:869–76.
23. Vogelzang NJ, Stadler WM. Kidney cancer. Lancet 1998;352:1691–6.
24. Medema RH, Kops GJ, Bos JL, Burgering BM. AFX-like Forkhead transcription factors mediate cell-cycle regulation by Ras and PKB through p27kip1. Nature 2000;404:782–7.
25. Luo J, Manning BD, Cantley LC. Targeting the PI3K-Akt pathway in human cancer: rationale and promise. Cancer Cell 2003;4:257–62.
26. Suyama K, Shapiro I, Guttman M, Hazan RB. A signaling pathway leading to metastasis is controlled by N-cadherin and the FGF receptor. Cancer Cell 2002;2:301–14.

Mod Rheumatol (2006) 16:3–13
DOI 10.1007/s10165-005-0452-4

REVIEW ARTICLE

Kei Ohnuma · Hiroshi Inoue · Masahiko Uchiyama
Tadanori Yamochi · Osamu Hosono · Nam H. Dang
Chikao Morimoto

T-cell activation via CD26 and caveolin-1 in rheumatoid synovium

Received: September 13, 2005 / Accepted: December 16, 2005

Abstract CD26 is a T-cell costimulatory molecule with dipeptidyl peptidase IV (DPPIV) activity in its extracellular region. We previously reported that recombinant soluble CD26 enhances peripheral blood T-cell proliferation induced by the recall antigen tetanus toxoid (TT). Recently, we demonstrated that CD26 binds caveolin-1 on antigen-presenting cell (APC), and that residues 201–211 of CD26 along with the serine catalytic site at residue 630, which constitute a pocket structure of CD26/DPPIV, contribute to binding to caveolin-1 scaffolding domain. In addition, following CD26–caveolin-1 interaction on TT-loaded monocytes, caveolin-1 is phosphorylated, with linkage to NF-κB activation, followed by upregulation of CD86. Finally, reduced caveolin-1 expression on APC inhibits CD26-mediated CD86 upregulation and abrogates CD26 effect on TT-induced T-cell proliferation, and immunohistochemical studies revealed an infiltration of CD26+ T cells in the sublining region of rheumatoid synovium and high expression of caveolin-1 in the increased vasculature and synoviocytes of the rheumatoid synovium. Taken together, these results strongly suggest that CD26–cavolin-1 interaction plays a role in the upregulation of CD86 on TT-loaded APC and subsequent engagement with CD28 on T cells, leading to antigen-specific T-cell activation such as the T-cell-mediated antigen-specific response in rheumatoid arthritis.

Key words Caveolin-1 · CD26 · Memory T cell · Rheumatoid arthritis (RA) · Synovial cell

K. Ohnuma · M. Uchiyama · T. Yamochi · O. Hosono · C. Morimoto (✉)
Department of Clinical Immunology, Advanced Clinical Research Center, Institute of Medical Science, University of Tokyo, 4-6-1 Shirokanedai, Minato-ku, Tokyo 108-8639, Japan
Tel. +81-354-495-546; Fax +81-354-495-448
e-mail: morimoto@ims.u-tokyo.ac.jp

H. Inoue
Inoue Hospital, Takasaki, Japan

N.H. Dang
Department of Hematologic Malignancies, Nevada Cancer Institute, Las Vegas, NV 89135, USA

Introduction

Rheumatoid arthritis (RA) is a chronic inflammatory disease characterized by the progressive destruction of cartilage and bone in the synovial joints, which is associated with proliferation of synovial cells and infiltration of activated memory T cells, antigen-presenting cells (APCs) and plasma cells.[1] Proposed etiologies for RA include genetic predisposition, dysregulation of self-tolerance, immune dysregulation triggered by environmental agents, and subsequent transformation of synovial cells.[1–3] Macrophages and/or T cells are important mediators of RA pathogenesis, with cytokines such as tumor necrosis factor alpha (TNF-α) and interleukin-1 (IL-1) being proven therapeutic targets. In fact, antagonists against such cytokines have been used recently as effective RA therapy, decreasing joint damage and slowing radiographic progression of disease in patients of RA with inadequate response to methotrexate.[4–7] However, as many patients do not experience effective relief even with the use of these newer biological agents, additional novel therapeutic approaches are still needed.[8–10]

Major-histocompatibility-complex (MHC) class II phenotype such as HLA-DR1, DR-4 and DR-14 confers susceptibility to RA.[11–14] MHC class II molecules present antigens to CD4+ T cells, suggesting an important role for T cells in the pathogenesis of RA. Moreover, the rheumatoid synovium contains activated T cells, providing further rationale for the proposal that T cells have an important role in RA.[15,16] Antigen-presenting cells such as monocytes, macrophages, and dendritic cells are also present in the rheumatoid synovium,[1] being activated and expressing both MHC class II and costimulatory molecules such as CD86 and CD80. These findings strongly suggest that the interaction between synovial T cells and APCs have a direct role in the progression of synovitis.[2] Moreover, careful analysis of infiltrating synovial T cells has revealed a bias towards the T_H1 phenotype.[17,18] In particular, patients with autoimmune diseases such as multiple sclerosis, Graves' disease, and RA have been found to have increased numbers of CD4+

CD26+ T cells in inflamed tissues as well as in their peripheral blood,[19–22] with enhancement of CD26 expression in these autoimmune diseases correlating with disease severity.[19,20,23] In addition, we previously demonstrated that T cells migrating through endothelial cell monolayers in vitro express high levels of CD26.[24] These findings imply that CD26+ T cells play an important role in the inflammation process and subsequent tissue damage in such diseases.

It is well established that T cells require at least two signals to be fully activated.[25] The first signal is antigen-specific and is delivered by engagement of the T-cell receptor (TCR) complex with an MHC-peptide complex on APC. The second signal is exerted by the binding of a costimulatory receptor on T cells to a ligand on the APCs. A key costimulatory signal is provided by the interaction of CD28 on T cells with CD86 or CD80 on APCs. We showed previously that CD26 on T cells have a very strong costimulatory effect on CD4+ T-cell activation in response to memory antigen such as tetanus toxoid (TT).[26–29] However, the molecular mechanism involved in the process of antigen-specific T-cell activation via CD26 has not been clearly elucidated. We recently demonstrated that caveolin-1 on antigen-loaded monocytes is a binding partner of CD26 and that signaling downstream of caveolin-1 in APC is triggered by stimulation with exogenous CD26.[30,31] Therefore, T-cell costimulation via CD26 as well as CD28 may have an important role in the pathophysiology of inflammatory diseases such as RA. In this review, we discuss various aspects of CD26 involvement in immune regulation and immune-mediated disorders such as RA, with a particular focus on the role of caveolin-1 as its key binding partner.

Structure and function of CD26

CD26 is a 110kDa cell-surface glycoprotein that belongs to the serine protease family, and human CD26 is expressed on a variety of tissues including T lymphocytes, endothelial and epithelial cells. As shown in Fig. 1A, human CD26 is composed of 766 amino acids, including a short cytoplasmic domain of 6 amino acids, a transmembrane region of 24 amino acids, and an extracellular domain with dipeptidyl peptidase activity which selectively removes the N-terminal dipeptide from peptides with proline or alanine at the penultimate position (dipeptidyl peptidase IV, DPPIV).[32] The amino acid sequence of human CD26 illustrates approximately 85% homology with the rat DPPIV enzyme and the mouse thymocyte activation molecule (THAM), the mouse homologue of human CD26.[33] CD26 knockout (CD26-KO) mice with C57BL/6 background display an apparently normal phenotype.[34,35] However, the percentage of CD4+ T cells is lower in the spleen lymphocyte population in the CD26-KO mice than in CD26-positive wild-type mice. After immunization of mice with PWM in vivo, serum levels of total IgG, IgG_1, IgG_{2a} and IgE were markedly decreased in CD26-KO mice than those in wild-type mice. Moreover, IL-4 and IL-2 level in sera of CD26-KO mice were decreased and production of interferon-gamma (IFN-γ) was delayed in response to PWM immunization. These results indicate that CD26 helps to regulate the development, maturation and migration of CD4+ T lymphocytes, cytokine secretion, T cell-dependent antibody production, and immunoglobulin isotype switching of B cells.[34]

In contrast to the function of murine CD26, human CD26+ T cells exert diverse effects.[28,36,37] CD26 is a membrane-associated ectopeptidase with DPPIV activity, and possible substrates of CD26/DPPIV include several critical cytokines and chemokines. Activity of RANTES (regulated on activation, normal T-cell expressed and secreted; CCL5) is altered by the enzymatic cleavage of DPPIV, as CD26/DPPIV-processed RANTES affects important activities such as those implicated in monocyte chemotaxis and HIV-1 infection.[38,39] Other important chemokines that appear to be substrates of DPPIV enzymatic activity include eotaxin (CCL11), macrophage-derived chemokine (MDC) (CCL22), interferon inducible chemokines (CXCL10), and other chemokines involved in the inhibition of HIV infection.[39] In addition, recent work showed that CD26 plays an important role in the mobilization of hematopoietic stem cell (HSC) and hematopoietic progenitor cells (HPC) induced by granulocyte colony-stimulating factor (G-CSF).[40] One of the substrates of CD26/DPPIV is CXCL12 (SDF-1α, stromal cell-derived factor 1 alpha), an important chemokine that serves as a chemoattractant for HSC/HPC.[41,42] It has been shown that CXCL12 can be selectively truncated in vitro by CD26/DPPIV, and the truncated molecule lacks the ability to induce migration of hematopoietic cells isolated from mouse bone marrow. Furthermore, treatment of mice with CD26/DPPIV inhibitors during the process of G-CSF mobilization results in a significant reduction in the number of mobilized HPC.[40,41] Other exciting development regarding DPPIV involves its role in glucose metabolism, since inhibition of endogenous glucagon-like peptide 1 (GLP-1) degradation by reducing DPPIV activity is an alternative strategy for improving the incretin action of GLP-1 in vivo and regulating glucose levels.[43] Selective small molecule inhibitors of DPPIV are currently being investigated in clinical trials for the treatment of impaired glucose tolerance and type 2 diabetes.[44]

Besides its ability to regulate the effect of biological factors through DPPIV enzyme activity, CD26 has an essential role in human T-cell physiology, especially in response to memory antigens (Fig. 1B).[28] Originally characterized as a T-cell differentiation antigen, CD26 is preferentially expressed on a specific population of T lymphocytes, the subset of CD4+ CD45RO+ memory T cells, and is upregulated following T-cell activation.[29] Besides being a marker of T-cell activation, CD26 is also associated with T-cell signal transduction processes as a costimulatory molecule.[27,37,45,46] In addition, CD26 serves as a functional collagen receptor with a role in T-cell activation, as well as having a potential role in thymic ontogeny (Fig. 2).[26,46,47] The enzymatic activity of CD26 appears to be very important in enhancing cellular responses to external stimuli. For example, Jurkat cells transfected with wild type CD26 consis-

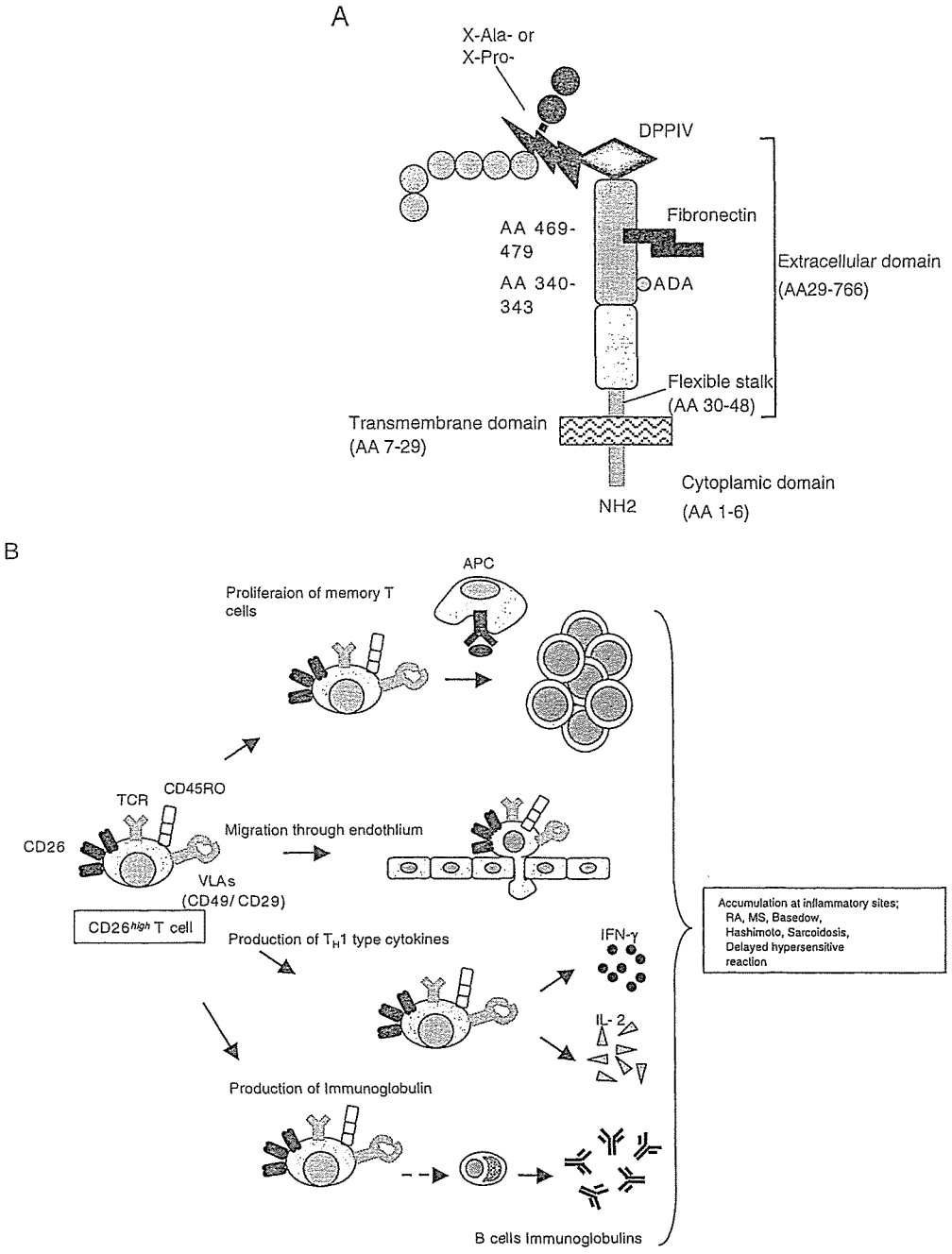

Fig. 1. **A** Schematic diagram of human CD26 structure. Adenosine deaminase (*ADA*) binding site at residues 340–343, fibronectin binding site at residue 469–479, and dipeptidyl peptidase IV (*DPPIV*) enzyme activity at Ser630. *X-Ala-* or *X-Pro-* denotes peptides containing any amino acid at N-terminal position with alanine or proline at the penultimate position. **B** Cellular function of $CD26^{high}$ T cell. See text for details. *APC*, antigen-presenting cell; *TCR*, T-cell receptor; *IFN*, interferon; *IL*, interleukin

tently demonstrate greater activation than parental CD26 negative Jurkat or cells transfected with CD26 mutated at the DPPIV enzymatic site.[48] Furthermore, CD26 interacts with several molecules playing important roles in T-cell function. CD26 physically binds with adenosine deaminase (ADA), an enzyme that plays a key role in the development and function of lymphoid tissues.[49–51] Adenosine deaminase is essential for purine metabolism, with the loss of ADA leading to a clinical syndrome characterized by severe immunodeficiency.[52] When the ADA inhibitor pentostatin was used in the treatment of recurrent T-cell lymphomas, a significant reduction in circulating CD26+ T cells was observed in treated patients.[53] This finding is consistent with the fact that there is a physical association between CD26 and ADA on the surface of T lymphocytes. CD26 also interacts with CD45RO, a tyrosine phosphatase with a critical role in T-cell signal transduction, at lipid rafts in peripheral blood T lymphocytes to modify cellular signaling events (Fig. 2).[54,55] Interestingly, CD26 is associated with CD45 RA outside of lipid rafts in cord blood T cells, and the strong physical linkage of CD26 and CD45 RA may be responsible for the attenuation of cord blood T-cell activation signaling through CD26, which may in turn result in immature immune response and the relatively low incidence of severe graft-versus-host disease (GVHD) in cord blood transplantation (Fig. 2).[56]

Since the 1970s, DPPIV-like activity has been reported in human serum. After identification of the ADA-binding

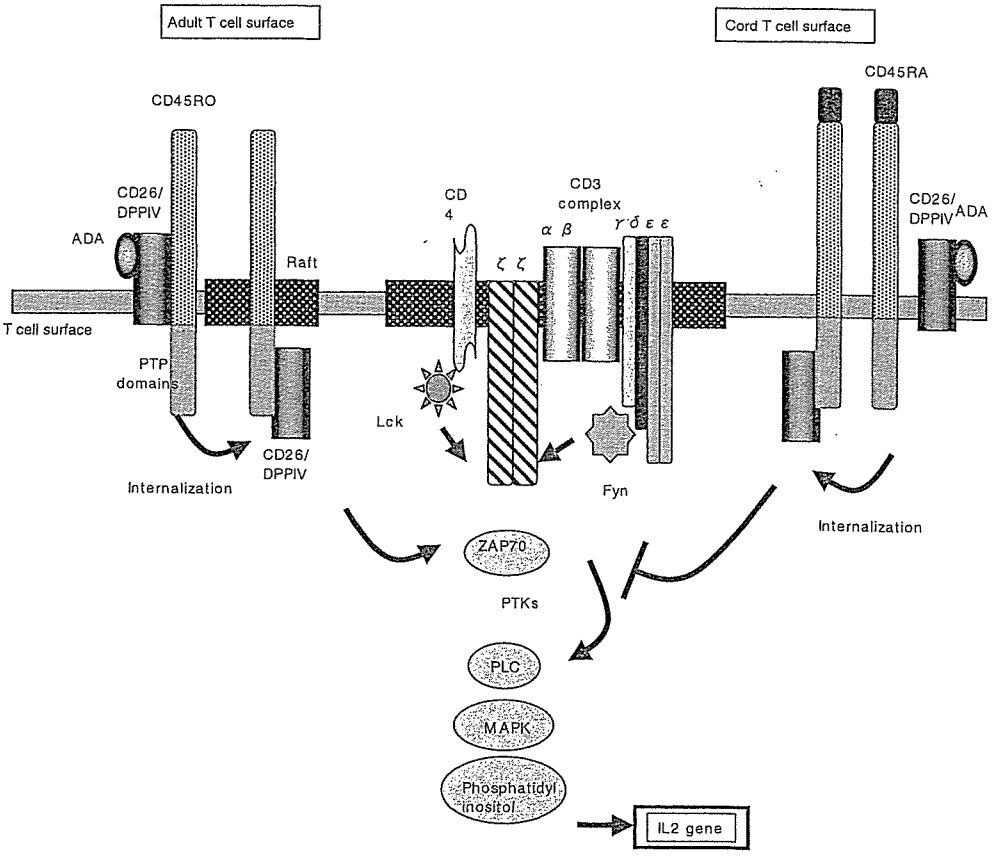

* the diagrams and models of molecules are not to scale.

Fig. 2. Schematic diagram of CD26-associated molecules in T-cell receptor-mediated activation of human adult peripheral blood T cell and cord blood T cell

protein of plasma as CD26, soluble form of CD26 protein was characterized in the serum and seminal fluids.[57,58] In the previous report, we have shown that exogenous recombinant soluble CD26 (rsCD26) enhances the proliferative response of peripheral blood lymphocytes (PBLs) to stimulation with the soluble antigen tetanus toxoid (TT).[59] More recently, we demonstrated that the target cells of rsCD26 are the CD14+ monocytes in the peripheral blood, and that rsCD26 upregulates CD86 expression, but not CD80 or HLA-DR antigen levels on monocytes.[30] Significantly, mannose 6-phosphate/insulin-like growth factor II receptor (M6P/IGF-IIR) was identified as a platform molecule for CD26 interaction with APC.[30] However, while both DPPIV-positive and DPPIV-negative rsCD26 are taken up by monocytes via M6P/IGF-IIR, only DPPIV-positive rsCD26 molecules affect CD86 upregulation on monocytes, thus suggesting that additional key factors may interact with CD26 in this process. We subsequently identified caveolin-1 on APC as a binding protein for CD26, and demonstrated that CD26 stimulation upregulates surface expression of CD86 on APC by means of caveolin-1 and enhances TT-mediated T-cell proliferation.[31] In the next section of this review, we will focus on caveolin-1 as the binding protein of CD26 in the context of antigen-driven T-cell activation.

Structure and function of caveolin-1

Caveolin-1 was the first family member discovered, and demonstrated as a structural component and marker for caveolae and trans-Golgi derived transport vesicles.[60,61] Caveolae were described as structures resembling "little caves" due to their appearance as 50- to 100-nm vesicular invaginations of the plasma membrane.[62] Caveolin-1 is expressed in a wide variety of cell types, especially terminally differentiated cells such as endothelial cells, adipocytes, alveolar type I pneumocytes, macrophages, synoviocytes, and smooth muscle cells. Presently, caveolin-related proteins have been identified as caveolin-1, -2, and -3, all of which serve as protein markers for caveolae.[63] The majority of caveolae in cells and tissues require only caveolin-1 expression for their proper formation, whereas caveolin-2 is not absolutely required, although the expression of caveolin-2 is tightly associated with the expression of caveolin-1.[64,65] On the other hand, caveolin-3 is found in skeletal muscle tissue and cardiac myocytes.[66] The three human genes encoding members of the caveolin family share significant homology. The caveolin-2 protein is approximately 38% identical and 58% similar to caveolin-1, while caveolin-3 is more closely related to caveolin-1, with 65% identity and 85% similarity.[63] All three caveolins possess an invariant "FEDVIAEP" stretch within their hydrophilic N-terminal domains which

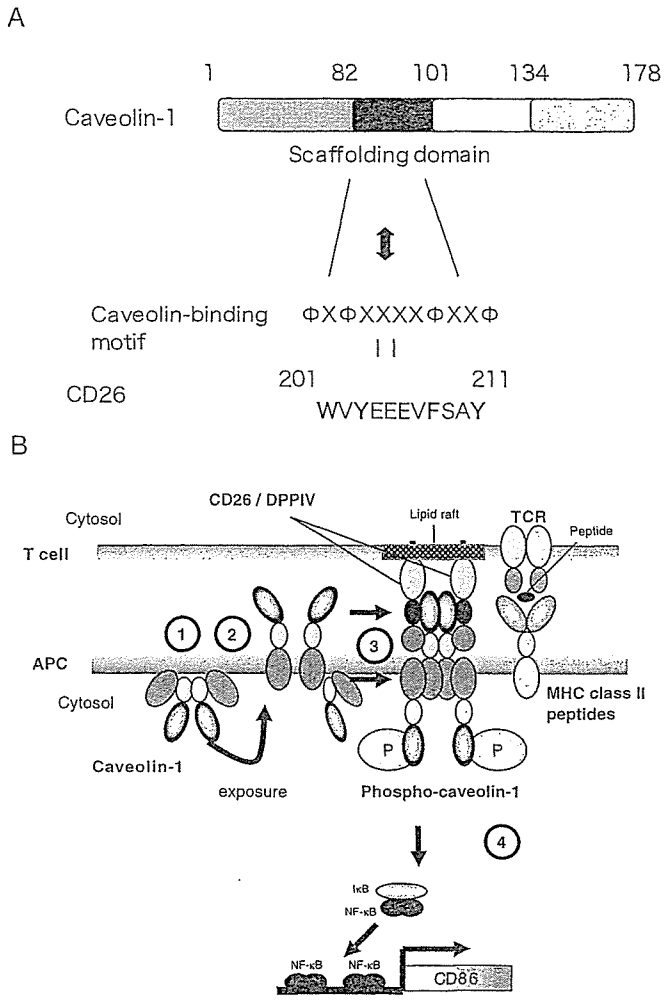

Fig. 3. **A** Schematic representation of human caveolin-1. Residues 1–81 comprise the N-terminal region (NT; *striped rectangle*), residues 82–101 comprise the scaffolding domain (SCD; *black rectangle*), residues 102–134 comprise the transmembrane region (memb; *open rectangle*), and residues 135–178 comprise the C-terminal region (*dotted rectangle*). CD26 contains a caveolin-binding motif (*ΦXΦXXXXΦXXΦ*; Φ and *X* depict aromatic residue and any amino acid, respectively), specifically WVYEEEVFSAY in CD26. **B** Model for CD26–caveolin-1 interaction leading to upregulation of CD86. *(1)* Caveolin-1 in monocytes (antigen-presenting cells; *APC*) resides at the inner membrane. *(2)* After uptake of tetanus toxoid into monocytes via caveolae, part of the population of caveolin-1 is exposed on the outer cell surface of tetanus toxoid (TT)-loaded monocytes. *(3)* Migration of CD26+ antigen-specific memory T cells to areas of antigen-loaded APCs results in contact with TT antigen-presenting APC, leading to the association of CD26 and caveolin-1. Aggregation of caveolin-1 in the contact area occurs, presumably by homo-oligomerization (via its residues 61–101), followed by its phosphorylation. *(4)* Phosphorylated caveolin-1 (*phospho-caveolin-1*) transduces signaling leading to activation of NF-κB, resulting in CD86 upregulation. *DPPIV*, dipeptidyl peptidase IV; *TCR*, T-cell receptor; *MHC*, major histocompatibility complex

are named the "caveolin signature motif."[67] Caveolin-1 is composed of 178 amino acid residues (Fig. 3A), and predominantly localized at the plasma membrane, demonstrating a punctuate staining patterns, and in Golgi-derived vesicles.[60] Two isoforms of caveolin-1 (caveolin-1α and β) have been identified, with the β-isoform composed of 31 residue truncated N-terminus of caveolin-1α isoform.[68] Caveolin-1 is composed of the N-terminal hydrophilic domain (residues 1–101), the oligomerization domain (residues 61–101), the scaffolding domain (SCD) (residues 82–101), the membrane spanning domain (residues 102–134), and the C-terminal lipid raft-anchoring domain (residues 135–178).[63] As in trans-Golgi transport, caveolin-1 plays an important role in signal transduction via its SCD, which compartmentalizes a multitude of signaling molecules.[63,69] These include G proteins, epidermal growth factor receptor, insulin receptor, endothelial nitric oxide synthase (eNOS), nonreceptor tyrosine kinase (Src, Fyn, Yes), flotillins, Ser/Thr kinases (PKA, Raf, MAPK, PI3K, Grb2), and catenins.[63,69] Other cellular functions of caveolin-1 are related to the lipid metabolism, especially to cholesterol scavenging in macrophages.[70] However, it is unknown whether caveolin-1 also plays a role in signal transduction in APCs. Although CD26 was present in caveolae of fibroblast-like synoviocytes,[71] direct CD26–cavolin-1 interaction and associated signaling events have not been demonstrated in immune cells. Interestingly, caveolin-1 knockout mice show defects in the angiogenic response to exogenous stimuli, such as Matrigel plugs containing angiogenic growth factors (bFGF) or tumors.[72] In this context, angiogenic vessels density and penetration was significantly reduced in caveolin-1 null mice. Moreover, electron microscopic examination revealed incomplete de novo capillary formation in tumors implanted within caveolin-1 null mice. Thus, it appears that caveolin-1 null mice have a defect in endothelial cell differentiation. This is consistent with in vitro observations demonstrating that overexpression of caveolin-1 enhances endothelial capillary-tube formation, while downregulation of caveolin-1 using an anti-sense approach blocks endothelial tube formation.[73] With regards to inflammation and caveolin-1, a series of elegant experiments showed that caveolin-1 has a role in inflammation with association of eNOS.[74] Using a cell permeable peptides link to the caveolin-1 scaffolding domain in aortic explants, the potent eNOS inhibiting activity of caveolin-1 was demonstrated. In vivo delivery of this peptide resulted in significant decreases in acute inflammation and edema resulting from vascular permeability. Taken together, these findings demonstrate an important relationship between caveolin-1 and vascularization, with implication for capillary formation in inflammatory processes.

Caveolin-1: CD26 binding protein in APC

Since CD26 on human T cells was identified as an activation antigen and costimulatory molecule of the TCR complex, several binding proteins to CD26 have been described. As described above, multiple chemokines interact with CD26/DPPIV as its substrates, and other proteins such as ADA, fibronectin, thromboxane A2 receptor, and CXCR4 are shown to be associated with CD26.[49,75–78] However, the precise mechanism involved in T-cell activation in response to memory antigen such as TT remains to be clearly characterized. Recently, we demonstrated that CD26 binds to

caveolin-1 on APC, and that residues 201–211 of CD26 along with the serine catalytic site at residue 630, which constitute a pocket structure of CD26/DPPIV, contribute to binding to the caveolin-1 scaffolding domain (Fig. 3A).[31] This region in CD26 contains a caveolin-binding domain (CBD) ($\Phi X\Phi XXXX\Phi XX\Phi$; Φ and X depict aromatic residue and any amino acid, respectively), specifically WVYEEEVFSAY in CD26.[48,69] These observations strongly support the notion that DPPIV enzyme activity is necessary to exert TCR-costimulatory activation via CD26.[48] In addition, following CD26–cavolin-1 interaction on TT-loaded monocytes, caveolin-1 is phosphorylated, with linkage to NF-κB activation, followed by upregulation of CD86. Finally, reduced caveolin-1 expression on monocytes inhibits CD26-mediated CD86 upregulation and abrogates CD26 effect on TT-induced T-cell proliferation (Fig. 3B). Taken together, these results strongly suggest that CD26–cavolin-1 interaction plays a role in the upregulation of CD86 on TT-loaded monocytes and subsequent engagement with CD28 on T cells, leading to antigen-specific T-cell activation.

Caveolin-1 has been reported to be an integral membrane protein with a cytoplasmic N-terminal domain and a cytoplasmic C-terminal domain.[63] Our data showed that the N-terminal domain of caveolin-1 was expressed on the cell surface of monocytes 12–24h after tetanus toxoid was loaded (Fig. 4A). Since tetanus toxoid was trafficked in cells through caveolae,[79,80] caveolin-1 may be transported along with the peptide-MHC complex in APC, and is then expressed on cell surface by the antigen-processing machinery for T-cell contact.[80–82] The data shown in Fig. 4B indicated that CD26 on activated memory T cells directly faces caveolin-1 on TT-loaded monocytes in the contact area, which is the immunological synapse for T cell-APC interaction. It is conceivable that the interaction of CD26 with caveolin-1 on antigen-loaded monocytes results in CD86 upregulation, therefore enhancing the subsequent interaction of CD86 and CD28 on T cells to induce antigen-specific T-cell proliferation and activation.

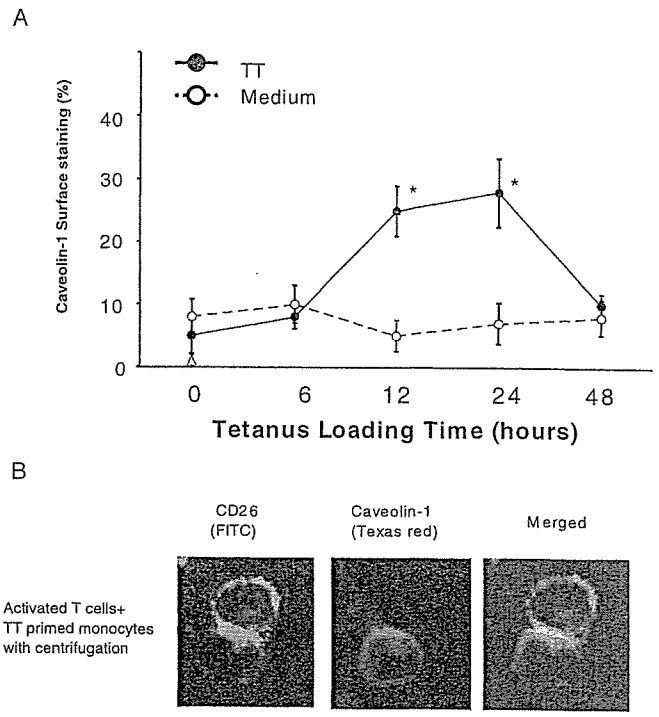

Fig. 4A,B. Immunocytochemical analysis of caveolin-1 and CD26 interaction. **A** Caveolin-1 in monocytes was exposed to cell surface after tetanus toxoid (*TT*) treatment, and interacted with CD26 on activated T cells. After purified monocytes were incubated with (*solid circle*) or without (*open circle*) TT, cell surface caveolin-1 was stained with anti-caveolin-1 antibody detecting the N terminal region, and analyzed for % positive cells by flow cytometry. Data of % positive cells represent mean ± SE from five independent experiments. *Asterisks* indicate points of significant increase. **B** To form cell–cell conjugation, activated T cells and TT-loaded monocytes were mixed, followed by centrifugation. Conjugates were fixed without permeabilization, and stained with anti-CD26 (fluorescein isothiocyanate) and anti-caveolin-1 (Texas red) antibodies. *Bars* 10μm

CD26 and caveolin-1 in synovitis

Rheumatoid arthritis is a classical example of an immune-mediated disease with chronically smoldering injury of the synovial joints resulting from infiltration of inflammatory cells, and synovitis of diarthrodial joints is its most visible manifestation. Although the observed architectures of rheumatoid synovitis vary in different individuals with RA as well as at various disease stages, the most frequent type of rheumatoid synovitis is a diffuse inflammatory infiltrate in which T cells, B cells, and macrophages are scattered around increased vasculature and synoviocytes. Meanwhile, in the remaining 40–50% of patients with RA, infiltrating inflammatory cells organize themselves into follicular structures.[1] It is known that the inflammatory activation events in rheumatoid synovitis are dependent upon cell–cell contact among T cells, fibroblast-like synoviocytes, APCs, and regional tissues such as type II collagen and proteoglycan.[83] Moreover, previous reports showed that CD26+ T cells exhibit strong migratory ability through endothelial cells, and are present at high levels in the rheumatoid synovium and the synovial fluids.[20,22,23] These findings suggest that T cells with high levels of CD26 antigen may preferentially migrate into the rheumatoid synovium to induce inflammation and tissue destruction. To test this hypothesis, we examined the expression of CD26 and caveolin-1 in the rheumatoid synovium through immunohistochemistry. As shown in Fig. 5A, CD26+ lymphoid cells are clearly observed in diffuse synovitis. In follicular synovitis examined with the sequential sections, CD26+ lymphoid cells are infiltrated in the sublining area of caveolin-1-positive synovial cells (arrow in panel b of Fig. 5B), and are adjacent to caveolin-1-positive inflammatory cells (arrowheads in panel c of Fig. 5B). Moreover, the intimal lining layer is hyperplastic with multiple layers, and the synoviocytes in these layers highly express caveolin-1 (arrow in Fig. 5C). In addition, CD86 and caveolin-1 are coexpressed in the intimal lining synoviocytes and the sublining fibroblast-like synovial cells (black arrowhead in Fig. 5C). Furthermore, increased vas-

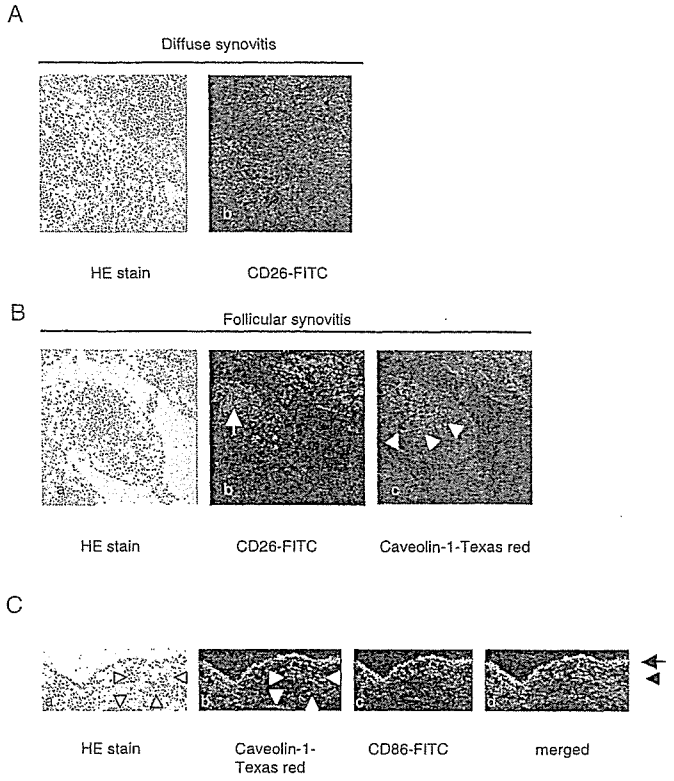

Fig. 5A–C. Architecture and immunohistochemistry of rheumatoid synovitis. **A** *Panel a* shows H&E-stained histology of diffuse synovitis with inflammatory cells intermingled with fibroblast-like synoviocytes (×100). *Panel b* shows immunohistochemistry of the sequential section of panel a, which was stained with fluorescein isothiocyanate (FITC)-conjugated anti-CD26 antibody (×100). **B** *Panel a* shows H&E-stained histology of follicular synovitis with germinal center formation (×100). *Panel b* shows immunohistochemistry of the sequential section of panel a, which was stained with FITC-conjugated anti-CD26 antibody. This reveals that CD26-positive lymphoid cells are scattered around the follicles (*arrow*) (×100). *Panel c* shows immunohistochemistry of the sequential section of panel b, which was stained with anti-caveolin-1 (Texas red). This reveals that the intimal lining synoviocytes and the sublining fibroblast-like synoviocytes adjacent to CD26+ lymphoid cells (arrow head) express caveolin-1 (×100). **C** *Panel a* shows synovial histology of rheumatoid arthritis with H&E staining (×100). *Panels b and c* show immunohistochemistry of the sequential section of panel a which was stained with caveolin-1 (Texas red) and CD86 (FITC), simultaneously. *Panel d* shows the merged view of panels b and c. *Arrow* shows the intimal lining synoviocytes, and *black arrowhead* shows the sublining fibroblast-like synoviocytes. *White arrowheads* show the increased vascularization in synovitis

cularization is seen in synovitis, and caveolin-1 is preferentially expressed in the luminar surface of endothelial cells in the rheumatoid synovium (white arrowheads in Fig. 5C). Taken together, we propose a model to describe the molecular events in monocytes leading to activation that are triggered by CD26–cavolin-1 interaction in rheumatoid synovium (Fig. 6). The initial step of inflammation in the synovium proceeds from activation of CD26+ T cells by APC and/or rheumatoid synoviocytes via presentation of a yet-to-be-identified antigen, concomitant with costimulation via such pairing as CD28–B7 and CD26–cavolin-1 (phase 1 in Fig. 6). With regard to the interaction between T cell–APC and the resultant immune response, entry of antigens via caveolae into APC leads to presentation of antigen peptides on MHC class II molecules and exposure of caveolin-1 (inside box in phase 1 of Fig. 6). APC thus induces the activation of memory T cells through the TCR and costimulatory molecules such as CD86/CD80–CD28, leading to the formation of mature immunological synapses. Following the association between caveolin-1 on APC and CD26 on memory T cells, CD86 is upregulated on APC surface, and memory T cells are subsequently activated via the costimulatory effect of CD26 on TCR activation. By enhancing TCR activation via CD26–cavolin-1 interaction, prolongation of the immunological synapse may be maintained. CD86 upregulation therefore results in potent T cell–APC interaction, leading to the development of activated memory T cells locally and activation of the immune response, as well as the subsequent development of rheumatoid synovitis. After triggering inflammation of the synovium, memory T-cell activation leads to progression of inflammation in rheumatoid synovium, i.e., infiltration of inflammatory cells, increase of vascular vessels, formation of follicular germinal centers, and proliferation of synoviocytes (phase 2 in Fig. 6). Destructive inflammation then progresses to cartilage and bone injury by pannus (phase 3 in Fig. 6). As a result, progressive inflammation leads to synovial membrane invasion of bone, loss of cartilage and bone destruction in joints.

Molecular-targeted therapeutic strategies in RA

Although the specific antigens responsible for the pathogenesis of RA have not been identified, T-cell activation via interaction with APCs plays a pivotal role in disease development. In this regard, therapeutic strategies have targeted cellular pathways in RA. In addition to anti-cytokine reagents, impressive therapeutic effect has been recently reported following the blocking of CD28-mediated costimulation by the use of cytotoxic T-lymphocyte-associated antigen 4-IgG1 (CTLA4Ig).[84,85] Expressed on T cells within hours to days after activation,[86,87] CTLA4 is the high-avidity receptor for both CD80 and CD86, and inhibits T-cell proliferation and IL-2 production.[88,89] A fusion protein, CTLA4Ig binds both CD80 and CD86 on APCs, thereby preventing these molecules from engaging CD28 on T cells.[90] By blocking the engagement of CD28, CTLA4Ig prevents the delivery of the second costimulatory signal that is required for optimal activation of T cells. The successful usage of this agent therefore demonstrates that blocking costimulatory signal to inhibit T-cell activation is a novel and promising therapeutic concept for selected autoimmune diseases.[84,85] In this regard, since we showed that CD26–cavolin-1 interaction may play a pivotal role in rheumatoid synovitis, reagents capable of blocking CD26–cavolin-1 interaction in synovitis may be potentially useful in the treatment of patients with RA.

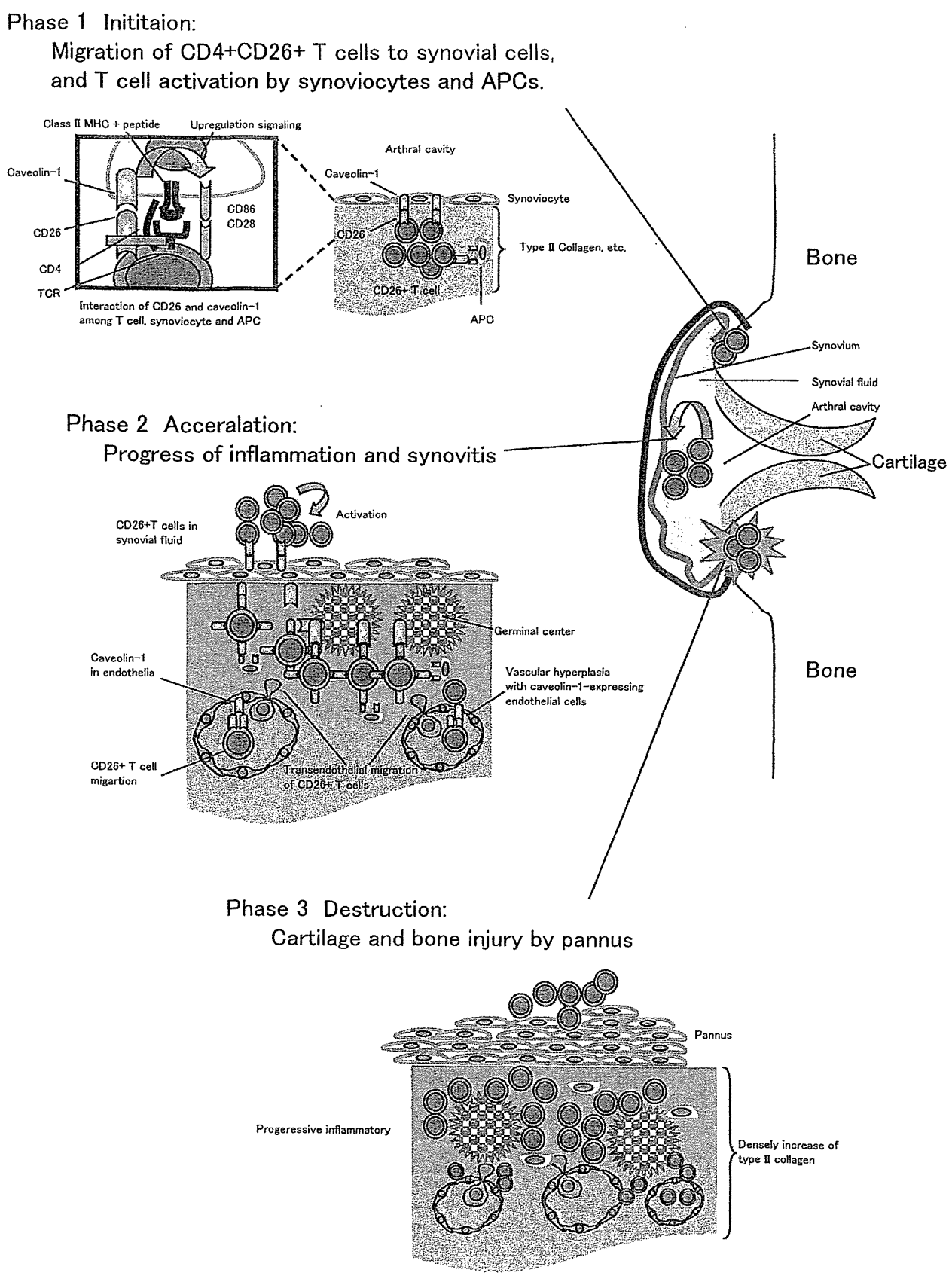

Fig. 6. Schematic diagram of inflammatory progress in rheumatoid synovitis. See text for details

Conclusions

Our results may thus provide a new approach to the treatment of autoimmune diseases or other immune-mediated disorders by directly intervening with the interaction between activated T-cell and APC. Targeting the binding of the pocket structure of CD26 and the scaffolding domain of caveolin-1 may lead to novel therapeutic approaches, including the utilization of antagonists that regulate antigen-specific immune response in immune-mediated disorders such as RA.

Acknowledgments This work was supported by Grants-in-Aid from the Ministry of Education, Science, Sports and Culture (K.O. and C.M.), and Ministry of Health, Labor, and Welfare, Japan (C.M.).

References

1. Goronzy JJ, Weyand CM. Rheumatoid arthritis. Immunol Rev 2005;204:55–73.
2. Mor A, Abramson SB, Pillinger MH. The fibroblast-like synovial cell in rheumatoid arthritis: a key player in inflammation and joint destruction. Clin Immunol 2005;115(2):118–28.
3. Yamada R, Tanaka T, Unoki M, Nagai T, Sawada T, Ohnishi Y, et al. Association between a single-nucleotide polymorphism in the promoter of the human interleukin-3 gene and rheumatoid arthritis in Japanese patients, and maximum-likelihood estimation of combinatorial effect that two genetic loci have on susceptibility to the disease. Am J Hum Genet 2001;68(3):674–85.
4. Elliott MJ, Maini RN, Feldmann M, Kalden JR, Antoni C, Smolen JS, et al. Randomised double-blind comparison of chimeric monoclonal antibody to tumour necrosis factor alpha (cA2) versus placebo in rheumatoid arthritis. Lancet 1994;344(8930):1105–10.
5. Bresnihan B, Alvaro-Gracia JM, Cobby M, Doherty M, Domljan Z, Emery P, et al. Treatment of rheumatoid arthritis with recombinant human interleukin-1 receptor antagonist. Arthritis Rheum 1998;41(12):2196–204.
6. Maini RN, Breedveld FC, Kalden JR, Smolen JS, Davis D, Macfarlane JD, et al. Therapeutic efficacy of multiple intravenous infusions of anti-tumor necrosis factor alpha monoclonal antibody combined with low-dose weekly methotrexate in rheumatoid arthritis. Arthritis Rheum 1998;41(9):1552–63.
7. Moreland LW, Baumgartner SW, Schiff MH, Tindall EA, Fleischmann RM, Weaver AL, et al. Treatment of rheumatoid arthritis with a recombinant human tumor necrosis factor receptor (p75)-Fc fusion protein. N Engl J Med 1997;337(3):141–7.
8. Bathon JM, Martin RW, Fleischmann RM, Tesser JR, Schiff MH, Keystone EC, et al. A comparison of etanercept and methotrexate in patients with early rheumatoid arthritis. N Engl J Med 2000;343(22):1586–93.
9. Lipsky PE, van der Heijde DM, St Clair EW, Furst DE, Breedveld FC, Kalden JR, et al. Infliximab and methotrexate in the treatment of rheumatoid arthritis. Anti-Tumor Necrosis Factor Trial in Rheumatoid Arthritis with Concomitant Therapy Study Group. N Engl J Med 2000;343(22):1594–602.
10. Moreland LW, Schiff MH, Baumgartner SW, Tindall EA, Fleischmann RM, Bulpitt KJ, et al. Etanercept therapy in rheumatoid arthritis. A randomized, controlled trial. Ann Intern Med 1999;130(6):478–86.
11. Nepom GT, Byers P, Seyfried C, Healey LA, Wilske KR, Stage D, et al. HLA genes associated with rheumatoid arthritis. Identification of susceptibility alleles using specific oligonucleotide probes. Arthritis Rheum 1989;32(1):15–21.
12. Gao XJ, Olsen NJ, Pincus T, Stastny P. HLA-DR alleles with naturally occurring amino acid substitutions and risk for development of rheumatoid arthritis. Arthritis Rheum 1990;33(7):939–46.
13. Nakai Y, Wakisaka A, Aizawa M, Itakura K, Nakai H, Ohashi A. HLA and rheumatoid arthritis in the Japanese. Arthritis Rheum 1981;24(5):722–5.
14. Ohta N, Nishimura YK, Tanimoto K, Horiuchi Y, Abe C, Shiokawa Y, et al. Association between HLA and Japanese patients with rheumatoid arthritis. Hum Immunol 1982;5(2):123–32.
15. Fox DA. The role of T cells in the immunopathogenesis of rheumatoid arthritis: new perspectives. Arthritis Rheum 1997;40(4):598–609.
16. Goronzy JJ, Weyand CM. T-cell regulation in rheumatoid arthritis. Curr Opin Rheumatol 2004;16(3):212–7.
17. Gracie JA, Forsey RJ, Chan WL, Gilmour A, Leung BP, Greer MR, et al. A proinflammatory role for IL-18 in rheumatoid arthritis. J Clin Invest 1999;104(10):1393–401.
18. Qin S, Rottman JB, Myers P, Kassam N, Weinblatt M, Loetscher M, et al. The chemokine receptors CXCR3 and CCR5 mark subsets of T cells associated with certain inflammatory reactions. J Clin Invest 1998;101(4):746–54.
19. Eguchi K, Ueki Y, Shimomura C, Otsubo T, Nakao H, Migita K, et al. Increment in the Ta1+ cells in the peripheral blood and thyroid tissue of patients with Graves' disease. J Immunol 1989;142(12):4233–40.
20. Gerli R, Muscat C, Bertotto A, Bistoni O, Agea E, Tognellini R, et al. CD26 surface molecule involvement in T-cell activation and lymphokine synthesis in rheumatoid and other inflammatory synovitis. Clin Immunol Immunopathol 1996;80(1):31–7.
21. Hafler DA, Fox DA, Manning ME, Schlossman SF, Reinherz EL, Weiner HL. In vivo activated T lymphocytes in the peripheral blood and cerebrospinal fluid of patients with multiple sclerosis. N Engl J Med 1985;312(22):1405–11.
22. Mizokami A, Eguchi K, Kawakami A, Ida H, Kawabe Y, Tsukada T, et al. Increased population of high fluorescence 1F7 (CD26) antigen on T cells in synovial fluid of patients with rheumatoid arthritis. J Rheumatol 1996;23(12):2022–6.
23. Muscat C, Bertotto A, Agea E, Bistoni O, Ercolani R, Tognellini R, et al. Expression and functional role of 1F7 (CD26) antigen on peripheral blood and synovial fluid T cells in rheumatoid arthritis patients. Clin Exp Immunol 1994;98(2):252–6.
24. Masuyama J, Berman JS, Cruikshank WW, Morimoto C, Center DM. Evidence for recent as well as long term activation of T cells migrating through endothelial cell monolayers in vitro. J Immunol 1992;148(5):1367–74.
25. Appleman LJ, Boussiotis VA. T cell anergy and costimulation. Immunol Rev 2003;192:161–80.
26. Dang NH, Torimoto Y, Shimamura K, Tanaka T, Daley JF, Schlossman SF, et al. 1F7 (CD26): a marker of thymic maturation involved in the differential regulation of the CD3 and CD2 pathways of human thymocyte activation. J Immunol 1991;147(9):2825–32.
27. Dang NH, Torimoto Y, Sugita K, Daley JF, Schow P, Prado C, et al. Cell surface modulation of CD26 by anti-1F7 monoclonal antibody. Analysis of surface expression and human T cell activation. J Immunol 1990;145(12):3963–71.
28. Morimoto C, Schlossman SF. The structure and function of CD26 in the T-cell immune response. Immunol Rev 1998;161:55–70.
29. Morimoto C, Torimoto Y, Levinson G, Rudd CE, Schrieber M, Dang NH, et al. 1F7, a novel cell surface molecule, involved in helper function of CD4 cells. J Immunol 1989;143(11):3430–9.
30. Ohnuma K, Munakata Y, Ishii T, Iwata S, Kobayashi S, Hosono O, et al. Soluble CD26/dipeptidyl peptidase IV induces T cell proliferation through CD86 up-regulation on APCs. J Immunol 2001;167(12):6745–55.
31. Ohnuma K, Yamochi T, Uchiyama M, Nishibashi K, Yoshikawa N, Shimizu N, et al. CD26 up-regulates expression of CD86 on antigen-presenting cells by means of caveolin-1. Proc Natl Acad Sci USA 2004;101(39):14186–91.
32. Tanaka T, Camerini D, Seed B, Torimoto Y, Dang NH, Kameoka J, et al. Cloning and functional expression of the T cell activation antigen CD26. J Immunol 1992;149(2):481–6.
33. Naquet P, MacDonald HR, Brekelmans P, Barbet J, Marchetto S, Van Ewijk W, et al. A novel T cell-activating molecule (THAM) highly expressed on CD4-CD8- murine thymocytes. J Immunol 1988;141(12):4101–9.

34. Yan S, Marguet D, Dobers J, Reutter W, Fan H. Deficiency of CD26 results in a change of cytokine and immunoglobulin secretion after stimulation by pokeweed mitogen. Eur J Immunol 2003;33(6):1519–27.
35. Marguet D, Baggio L, Kobayashi T, Bernard AM, Pierres M, Nielsen PF, et al. Enhanced insulin secretion and improved glucose tolerance in mice lacking CD26. Proc Natl Acad Sci USA 2000;97(12):6874–9.
36. Fleischer B. CD26: a surface protease involved in T-cell activation. Immunol Today 1994;15(4):180–4.
37. von Bonin A, Huhn J, Fleischer B. Dipeptidyl-peptidase IV/CD26 on T cells: analysis of an alternative T-cell activation pathway. Immunol Rev 1998;161:43–53.
38. Oravecz T, Pall M, Roderiquez G, Gorrell MD, Ditto M, Nguyen NY, et al. Regulation of the receptor specificity and function of the chemokine RANTES (regulated on activation, normal T cell expressed and secreted) by dipeptidyl peptidase IV (CD26)-mediated cleavage. J Exp Med 1997;186(11):1865–72.
39. Proost P, Struyf S, Schols D, Opdenakker G, Sozzani S, Allavena P, et al. Truncation of macrophage-derived chemokine by CD26/dipeptidyl-peptidase IV beyond its predicted cleavage site affects chemotactic activity and CC chemokine receptor 4 interaction. J Biol Chem 1999;274(7):3988–93.
40. Christopherson KW, 2nd, Hangoc G, Mantel CR, Broxmeyer HE. Modulation of hematopoietic stem cell homing and engraftment by CD26. Science 2004;305(5686):1000–3.
41. Christopherson KW, Cooper S, Hangoc G, Broxmeyer HE. CD26 is essential for normal G-CSF-induced progenitor cell mobilization as determined by CD26-/- mice. Exp Hematol 2003;31(11):1126–34.
42. Christopherson KW, 2nd, Hangoc G, Broxmeyer HE. Cell surface peptidase CD26/dipeptidylpeptidase IV regulates CXCL12/stromal cell-derived factor-1 alpha-mediated chemotaxis of human cord blood CD34+ progenitor cells. J Immunol 2002;169(12):7000–8.
43. Wiedeman PE, Trevillyan JM. Dipeptidyl peptidase IV inhibitors for the treatment of impaired glucose tolerance and type 2 diabetes. Curr Opin Invest Drugs 2003;4(4):412–20.
44. Ristic S, Byiers S, Foley J, Holmes D. Improved glycaemic control with dipeptidyl peptidase-4 inhibition in patients with type 2 diabetes: vildagliptin (LAF237) dose response. Diabetes Obes Metab 2005;7(6):692–8.
45. Dang NH, Torimoto Y, Deusch K, Schlossman SF, Morimoto C. Comitogenic effect of solid-phase immobilized anti-1F7 on human CD4 T cell activation via CD3 and CD2 pathways. J Immunol 1990;144(11):4092–100.
46. Dang NH, Torimoto Y, Schlossman SF, Morimoto C. Human CD4 helper T cell activation: functional involvement of two distinct collagen receptors, 1F7 and VLA integrin family. J Exp Med 1990;172(2):649–52.
47. Ruiz P, Zacharievich N, Hao L, Viciana AL, Shenkin M. Human thymocyte dipeptidyl peptidase IV (CD26) activity is altered with stage of ontogeny. Clin Immunol Immunopathol 1998;88(2):156–68.
48. Tanaka T, Kameoka J, Yaron A, Schlossman SF, Morimoto C. The costimulatory activity of the CD26 antigen requires dipeptidyl peptidase IV enzymatic activity. Proc Natl Acad Sci USA 1993;90(10):4586–90.
49. Kameoka J, Tanaka T, Nojima Y, Schlossman SF, Morimoto C. Direct association of adenosine deaminase with a T cell activation antigen, CD26. Science 1993;261(5120):466–9.
50. Dong RP, Kameoka J, Hegen M, Tanaka T, Xu Y, Schlossman SF, et al. Characterization of adenosine deaminase binding to human CD26 on T cells and its biologic role in immune response. J Immunol 1996;156(4):1349–55.
51. Dong RP, Tachibana K, Hegen M, Munakata Y, Cho D, Schlossman SF, et al. Determination of adenosine deaminase binding domain on CD26 and its immunoregulatory effect on T cell activation. J Immunol 1997;159(12):6070–6.
52. Goldblum RM, Schmalstieg FC, Nelson JA, Mills GC. Adenosine deaminase (ADA) and other enzyme abnormalities in immune deficiency states. Birth Defects Orig Artic Ser 1978;14(6A):73–84.
53. Dang NH, Hagemeister FB, Duvic M, Romaguera JE, Younes A, Jones D, et al. Pentostatin in T-non-Hodgkin's lymphomas: efficacy and effect on CD26+ T lymphocytes. Oncol Rep 2003;10(5):1513–8.
54. Torimoto Y, Dang NH, Vivier E, Tanaka T, Schlossman SF, Morimoto C. Coassociation of CD26 (dipeptidyl peptidase IV) with CD45 on the surface of human T lymphocytes. J Immunol 1991;147(8):2514–7.
55. Ishii T, Ohnuma K, Murakami A, Takasawa N, Kobayashi S, Dang NH, et al. CD26-mediated signaling for T cell activation occurs in lipid rafts through its association with CD45RO. Proc Natl Acad Sci USA 2001;98(21):12138–43.
56. Kobayashi S, Ohnuma K, Uchiyama M, Iino K, Iwata S, Dang NH, et al. Association of CD26 with CD45RA outside lipid rafts attenuates cord blood T-cell activation. Blood 2004;103(3):1002–10.
57. Iwaki-Egawa S, Watanabe Y, Kikuya Y, Fujimoto Y. Dipeptidyl peptidase IV from human serum: purification, characterization, and N-terminal amino acid sequence. J Biochem (Tokyo) 1998;124(2):428–33.
58. Durinx C, Lambeir AM, Bosmans E, Falmagne JB, Berghmans R, Haemers A, et al. Molecular characterization of dipeptidyl peptidase activity in serum: soluble CD26/dipeptidyl peptidase IV is responsible for the release of X-Pro dipeptides. Eur J Biochem 2000;267(17):5608–13.
59. Tanaka T, Duke-Cohan JS, Kameoka J, Yaron A, Lee I, Schlossman SF, et al. Enhancement of antigen-induced T-cell proliferation by soluble CD26/dipeptidyl peptidase IV. Proc Natl Acad Sci USA 1994;91(8):3082–6.
60. Glenney JR Jr. Tyrosine phosphorylation of a 22-kDa protein is correlated with transformation by Rous sarcoma virus. J Biol Chem 1989;264(34):20163–6.
61. Rothberg KG, Heuser JE, Donzell WC, Ying YS, Glenney JR, Anderson RG. Caveolin, a protein component of caveolae membrane coats. Cell 1992;68(4):673–82.
62. Yamada E. The fine structure of the gall bladder epithelium of the mouse. J Biophys Biochem Cytol 1955;1(5):445–58.
63. Smart EJ, Graf GA, McNiven MA, Sessa WC, Engelman JA, Scherer PE, et al. Caveolins, liquid-ordered domains, and signal transduction. Mol Cell Biol 1999;19(11):7289–304.
64. Razani B, Engelman JA, Wang XB, Schubert W, Zhang XL, Marks CB, et al. Caveolin-1 null mice are viable but show evidence of hyperproliferative and vascular abnormalities. J Biol Chem 2001;276(41):38121–38.
65. Razani B, Wang XB, Engelman JA, Battista M, Lagaud G, Zhang XL, et al. Caveolin-2-deficient mice show evidence of severe pulmonary dysfunction without disruption of caveolae. Mol Cell Biol 2002;22(7):2329–44.
66. Galbiati F, Engelman JA, Volonte D, Zhang XL, Minetti C, Li M, et al. Caveolin-3 null mice show a loss of caveolae, changes in the microdomain distribution of the dystrophin-glycoprotein complex, and t-tubule abnormalities. J Biol Chem 2001;276(24):21425–33.
67. Scherer PE, Okamoto T, Chun M, Nishimoto I, Lodish HF, Lisanti MP. Identification, sequence, and expression of caveolin-2 defines a caveolin gene family. Proc Natl Acad Sci USA 1996;93(1):131–5.
68. Scherer PE, Tang Z, Chun M, Sargiacomo M, Lodish HF, Lisanti MP. Caveolin isoforms differ in their N-terminal protein sequence and subcellular distribution. Identification and epitope mapping of an isoform-specific monoclonal antibody probe. J Biol Chem 1995;270(27):16395–401.
69. Couet J, Li S, Okamoto T, Ikezu T, Lisanti MP. Identification of peptide and protein ligands for the caveolin-scaffolding domain. Implications for the interaction of caveolin with caveolae-associated proteins. J Biol Chem 1997;272(10):6525–33.
70. Gargalovic P, Dory L. Caveolins and macrophage lipid metabolism. J Lipid Res 2003;44(1):11–21.
71. Riemann D, Hansen GH, Niels-Christiansen L, Thorsen E, Immerdal L, Santos AN, et al. Caveolae/lipid rafts in fibroblast-like synoviocytes: ectopeptidase-rich membrane microdomains. Biochem J 2001;354(Pt 1):47–55.
72. Woodman SE, Ashton AW, Schubert W, Lee H, Williams TM, Medina FA, et al. Caveolin-1 knockout mice show an impaired angiogenic response to exogenous stimuli. Am J Pathol 2003;162(6):2059–68.
73. Liu J, Wang XB, Park DS, Lisanti MP. Caveolin-1 expression enhances endothelial capillary tubule formation. J Biol Chem 2002;277(12):10661–8.